



CHALMERS
UNIVERSITY OF TECHNOLOGY



Battery Storage for Charging, Grid Support and Island Operation in the Port of Gothenburg

Case Study: Island Operation in the Port of Gothenburg

Master's thesis in Electric Power Engineering

Andreas Benjaminsson

Department of Electrical Engineering
CHALMERS UNIVERSITY OF TECHNOLOGY
Gothenburg, Sweden 2022
www.chalmers.se

MASTER'S THESIS 2022

Battery Storage for Charging, Grid Support and Island Operation in the Port of Gothenburg

Case Study: Island Operation in the Port of Gothenburg

Andreas Benjaminsson



CHALMERS
UNIVERSITY OF TECHNOLOGY

Division of Electric Power Engineering
Department of Electrical Engineering
CHALMERS UNIVERSITY OF TECHNOLOGY
Gothenburg, Sweden 2022

Battery Storage for Charging, Grid Support and Island Operation in the Port of
Gothenburg
Case Study: Island Operation in the Port of Gothenburg
Andreas Benjaminsson

© Andreas Benjaminsson, 2022.

Supervisor: Lucas Thomée, Team Lead at DNV
Supervisors: Massimo Bongiorno & Anant Narula
Examiner: Massimo Bongiorno, Department of Electrical Engineering

Master's Thesis 2022
Division of Electric Power Engineering
Department of Electrical Engineering
Chalmers University of Technology
SE-412 96 Gothenburg
Telephone +46 31 772 1000

Cover: Visualisation of Arendal, Port of Gothenburg with the future Stena Elektra
berthed [1].

Typeset in L^AT_EX
Printed by Chalmers Reproservice
Gothenburg, Sweden 2022

Battery Storage for Charging, Grid Support and Island Operation in the Port of Gothenburg

Case Study: Island Operation in the Port of Gothenburg

Andreas Benjaminsson

Department of Electrical Engineering

Chalmers University of Technology

Abstract

Environmental impacts of human actions have shown severe long-term consequences. In order to mitigate this effect, the current trend is a conversion from non-renewable sources of energy to substitutes that are more sustainable. The EU-funded project Sea Li-ion was initiated with the specific target of accelerating maritime electrification. The project investigates the idea of using Battery Energy Storage Systems (BESS) in harbour areas with the primary application of charging electric ferries.

Using the onshore BESS for charging of electric ferries alone limits the possible benefits of such a configuration. BESS can be used to provide ancillary grid services to increase system stability in frequency and voltage magnitude, as well as assist during times of high loading. Furthermore, it can be used in an islanded system configuration where a section of the power system is disconnected from the synchronous grid. This becomes particularly important should the main grid be subject to major disturbance or outage.

This thesis investigates how a BESS can be used to support an isolated grid. An islanded grid is modelled around the Port of Gothenburg, consisting of gas turbines from Rya combined heat and power plant, BESS and an electric ferry representing a load. The gas turbines serve as primary generation for the grid whereas the BESS impact on the grid performance is investigated.

The BESS is modelled as a battery connected to a grid-forming converter as an interface to the islanded grid. A suitable control system is developed where the impact of different control parameters is investigated. The system performance without the BESS and with the BESS installed is assessed to investigate the impact of a BESS in an islanded system configuration.

Results show that the BESS possesses fast dynamics and can be efficiently used with conventional generating units to improve the initial frequency response during an event on the grid. Frequency oscillations can be mitigated by configuring the BESS control accordingly. BESS provides a major benefit of having a control structure that allows specific tuning, which can be used to target requirements of the grid in question.

Keywords: Sea Li-ion, Battery Energy Storage System (BESS), Second-life lithium-ion batteries, Electric ferry, Port of Gothenburg, Island operation, Grid-forming converter, Frequency support.

Acknowledgements

I would like to express special gratitude to my supervisor Lucas Thomée at DNV for providing helpful guidance, discussions and suggestions to elevate the outcome of the thesis. Further, acknowledgement and gratefulness towards my supervisors Massimo Bongiorno and Anant Narula from Chalmers is in place for providing significant background material for the thesis and for promoting critical thinking throughout the process. Additionally, I want to express my sincerest appreciation to the employees at DNV who has partaken in the thesis, with special emphasis to Arvid Björemark for his assistance in the process of learning PowerFactory.

Andreas Benjaminsson, Gothenburg, June 2022

Contents

List of Figures	xiii
List of Tables	xvii
1 Introduction	1
1.1 Background	1
1.2 Purpose	2
1.3 Scope	2
1.4 Report Structure	3
2 Characteristics of Electric Ferry, Harbour and Rya CHP	5
2.1 Electric Ferry	5
2.2 Harbour Loads	7
2.3 Harbour Connection to Main Grid	7
2.4 Rya CHP Plant	8
3 Analysed Power System and Grid Requirements	11
3.1 Overview of Investigated Power System	11
3.1.1 Geographical Orientation of Considered Grid Units	11
3.1.2 Analysed Power System Setup	12
3.1.2.1 Grid-Connected System Setup	12
3.1.2.2 Islanded System Setup	13
3.2 Grid Requirements	14
3.2.1 Voltage Requirements	14
3.2.2 Frequency Requirements	15
3.2.3 Generator Requirements	16
3.3 Frequency Regulating Services	17
4 Battery Energy Storage Systems	19
4.1 BESS for Power System Applications	19
4.2 BESS Structure	20
4.3 Electrical Modelling of Lithium-Ion Batteries	20
4.3.1 Equivalent Circuit Model Representation	21
4.3.2 Temperature	23
4.3.3 State of Charge	23
4.3.4 Capacity and Power Fade	24
4.4 Impacts of Second-Life Batteries	24

5	Converters and Control Concepts	27
5.1	Converter Control Structures	27
5.1.1	Grid-Following Converter	27
5.1.2	Grid-Forming Converter	27
5.2	Converter Control Concepts	28
5.2.1	System Model for Control Derivation	28
5.2.2	Power Synchronization Control	28
5.2.3	Virtual Synchronous Machine	30
5.2.4	Active Power Control with PI-Controller	32
5.2.5	Voltage Control	34
5.2.6	Frequency Control	35
6	System Realization	37
6.1	Battery Modelling	37
6.2	BESS Representation	38
6.3	Control System Setup	38
6.4	Modelling of Gas Turbines in Rya CHP Plant	39
6.5	Verification of Model Implementations	40
6.5.1	Battery Model Verification	40
6.5.2	BESS Control System Verification	41
6.5.2.1	Effect of Active Damping from Measured Power . . .	42
6.5.2.2	Effect of Active Damping from Measured Current . .	43
7	Simulation Models and Case Studies	45
7.1	Overview of Simulation Cases	45
7.2	Grid-Connected Model and Case Studies	45
7.2.1	Simulation Models for Grid-Connected Operation	46
7.2.2	Grid-Connected Charging of Ferry	47
7.3	Simulation Model and Case Studies for Islanded Operation	48
7.3.1	Simulation Model for Islanded Operation	48
7.3.2	Islanded Charging of Ferry	49
7.3.3	Frequency Response Improvement	50
7.3.4	Impacts of Reaching SOC Limits	50
7.3.5	Frequency Controller Gain	50
7.3.6	BESS Virtual Inertia Constant	50
8	Simulation Results	53
8.1	Connection of Electric Ferry to Main Grid	53
8.1.1	Synchronous System Frequency for Electric Ferry Connection	53
8.1.2	Connection of Electric Ferry to Estimated Grid Strength . . .	54
8.1.3	Connection of Electric Ferry to Weak Grid	55
8.2	Connection of Electric Ferry to Islanded Grid	55
8.2.1	Fast Connection of Electric Ferry	55
8.2.2	Slow Connection of Electric Ferry	58
8.3	State of Charge Limits	60
8.3.1	Lower SOC Limit and Charge Initiation	60
8.3.2	Maximum SOC Limit and Support Initialization	61

8.4	System Response with Alternative Frequency Controller	62
8.5	Impact of Frequency Controller Gain	63
8.6	Impact of BESS Inertia Constant	65
9	Discussion	67
9.1	BESS for Reducing Main Grid Impact	67
9.2	BESS for Islanded Operation	68
9.3	Islanded System Demand of BESS	70
9.4	BESS or Grid Extension for Environmental Profits	70
9.5	Future Work	71
9.5.1	Converter Model	71
9.5.2	Black-Start and Seamless Transfer of Islanded Grid	71
9.5.3	BESS Behaviour During Faults	72
10	Conclusion	73
	Bibliography	75
A	Rya Gas Turbine Verification	I

List of Figures

2.1	Illustration of the electric ferry Stena Elektra. Image provided by Stena Mediabank [13].	5
3.1	Geographical representation of harbour components for power system. This includes the placement of the electric ferry, BESS, Substation, Rya CHP and a simplified representation of the 10 and 130 kV cables.	12
3.2	Illustration of Arendal with Stena Elektra berthed in the harbour provided from [1].	12
3.3	Diagram representation of investigated power system from the perspective of the harbour. The external grid is modelled as an aggregated model of the total generation and load of the synchronous grid.	13
3.4	Diagram representation of investigated islanded power system from The model consists of the harbour with the electric ferry, the BESS, gas turbines in Rya as well as the harbour substation interface.	14
3.5	Generation unit characteristic for active power output versus frequency. If the measured frequency is within the deadband, the corresponding change in active power output ΔP is zero. When the frequency is outside the deadband, the active power output is a linear function of the frequency deviation. The nominal system frequency is marked and expressed as f_{nom}	16
3.6	Measured system frequency on 2022-03-01 during the time of 06:00-07:00, as well as indications of normal allowed frequency deviations from the nominal [23]. Frequency data on the official SVK website is provided by Statnett.	16
4.1	Generic structure of a grid-connected BESS. The primary elements are the battery, converter, BMS and converter controller. The BMS monitors the corresponding battery packs within the battery to ensure safe and reliable operation, while the converter controller decides the BESS power exchange with the corresponding power system.	20
4.2	Equivalent circuit models of lithium-ion batteries with increasing complexity. The most trivial model (Figure 4.2(a)) consists of an OCV in series with a pure resistance to account for the internal voltage drop of the battery. Higher order models (Figure 4.2(b) and Figure 4.2(c)) include parallel RC branches to represent polarization processes and hence present a more dynamically accurate battery model.	22

5.1	Simplified network model used for derivation of control concepts for grid-forming converter. The model consists of a voltage source representing the BESS with a series RL-filter Z_f as well as the overlying grid, together with the grid equivalent impedance Z_g	28
5.2	Block diagram of basic PSC structure, consisting of proportional control parameter K_p and the corresponding transfer function between θ and P , expressed as $J_{P\theta}(s)$ [54].	29
5.3	Block diagram of PSC control structure with active damping from measured current from [55].	30
5.4	Block diagram for PSC with K_p replaced by swing equation. The system transfer function between θ and P is expressed as $\frac{V_c V_g}{X_f}$	31
5.5	Block diagram of active power controller, constituted by a PI-controller that takes measured active power and active power reference as input. A damping term R_{a1} is added to reduce overshoots in active power output when a reference power is given to the control system.	33
5.6	Block diagram of active power control with PI-controller.	33
5.7	Block diagram of voltage controller that keeps the voltage at the PCC close to the nominal voltage. The controller compares the measured PCC voltage magnitude in dq-frame with the nominal voltage magnitude.	35
5.8	Block diagram of frequency controller to provide reference active power setpoint for BESS control system. The control system takes the measured system frequency and compares it to the reference frequency to set the corresponding reference active power.	36
5.9	Block diagram of adjusted frequency controller with high-pass filter to slowly set the adjusted output active power of the BESS due to a frequency deviation to zero after an event.	36
6.1	Mathematical representation of the battery model. The measured current and temperature are taken as input, where in turn the SOC and resulting battery terminal voltage are found.	38
6.2	Representation of full control system for BESS. This includes measurements of active power, currents and voltages. The measured quantities are transformed to $\alpha\beta$ -frame and dq -frame, and fed to the corresponding control system models.	39
6.3	Battery SOC-profile, current, OCV and terminal voltage for 1C discharge and charge in a SOC range of 0.9–0.1.	41
6.4	Testing system for BESS control consisting of BESS, converter filter and grid.	42
6.5	Control system response when active power reference is stepped from 0 to 1 p.u. and vice versa for grid strengths with SCR = 2, SCR = 10 and SCR = 20.	42
6.6	Response of BESS when an active power step of 1 p.u. is applied and removed with and without the damping term R_{a1} from the measured power.	43

6.7	Response of BESS when an active power step of 1 p.u. is applied and removed with and without the damping term R_a from the measured current.	44
7.1	One-line diagram for grid-connected operation for frequency response analysis. The grid consists of an aggregated hydropower plant, BESS, electric ferry and aggregated loads.	46
7.2	One-line diagram for grid-connected operation for Voltage magnitude analysis. The grid consists of an external grid, BESS, electric ferry and aggregated loads.	47
7.3	One-line diagram for islanded grid used for simulations in PowerFactory, consisting of BESS together with the BESS converter filter as well as gas turbines, electric ferry and aggregated loads.	49
8.1	Synchronous system frequency when the external grid is modelled as an aggregated hydropower plant and the electric ferry is connected.	54
8.2	Voltage magnitude at electric ferry connection point when external grid strength is chosen according to data from [65].	54
8.3	Voltage magnitude at harbour connection point when the electric ferry is connected to a weak external grid.	55
8.4	Change in electric and mechanical power output of gas turbine, load power of the electric ferry, as well as system frequency response and voltage magnitude at ferry bus for connection of electric ferry when BESS is not present during a fast connection strategy.	56
8.5	Change in electric and mechanical power output of gas turbine, BESS electric power, load power of electric ferry, as well as system frequency response and voltage magnitude at ferry bus for connection of electric ferry when BESS is present during a fast connection strategy.	57
8.6	System response comparison for islanded power system when BESS is not present and when BESS is used for frequency support during a fast connection strategy.	58
8.7	Change in electric and mechanical power output of gas turbine, load power of the electric ferry, as well as system frequency response and voltage magnitude at ferry bus for connection of electric ferry when BESS is not present during a slow connection strategy.	59
8.8	Change in electric and mechanical power output of gas turbine, BESS electric power, load power of electric ferry, as well as system frequency response and voltage magnitude at ferry bus for connection of electric ferry when BESS is present during a slow connection strategy.	59
8.9	System response comparison for islanded power system when BESS is not present and when BESS is used for frequency support during a slow connection strategy.	60
8.10	Change in electric and mechanical power output of gas turbine, electric power of BESS, system frequency and BESS SOC when minimum SOC is reached and charging is initiated.	61

8.11	Change in gas turbine electric and mechanical power, BESS electric power, system frequency and BESS SOC when Maximum SOC is reached and support is initiated.	62
8.12	Gas turbine electric and mechanical power, BESS electric power and system frequency comparison for the original and adjusted frequency controller.	63
8.13	Battery SOC and terminal voltage comparison for original and adjusted frequency controller.	63
8.14	Electric and mechanical power output of gas turbines, active power of BESS as well as system frequency when the electric ferry is connected as a ramp over one second from zero to nominal load with BESS frequency controller gain of 25 and 100.	64
8.15	SOC and battery terminal voltage when the electric ferry is connected as a ramp over one second from zero to nominal load with BESS frequency controller gain of 25 and 100.	65
8.16	Active power output of BESS and system frequency for virtual inertia constant of $H = 5$ s, $H = 10$ s, $H = 20$ s and $H = 30$ s.	66
A.1	Active power output for gas turbine and load active power, as well as system frequency. Initially, the gas turbine is supplying a load of 100 MW, and at the time of 5 seconds, 15 MW load is suddenly lost, causing the gas turbine to reduce its output active power and increase the corresponding frequency.	I

List of Tables

2.1	Seasonal schedule of electric ferry Stena Elektra. During peak season, the expected schedule is that the electric ferry travels six times per day, whereas it is only expected to travel four times per day in the low season.	6
2.2	Additional loads as well as power requirement in comparison to Stena Elektra as a consequence of the electric ferry installation. This includes energy to power the terminal, freight houses and quay lighting.	7
3.1	Required operation times for generating units connected to the Nordic synchronous system [24]. The frequency range of 49.0 – 51.0 Hz is considered the norm where continuous operation is expected. Outside of this frequency range, generating units are only required to properly function for a limited time period.	17
6.1	GAST governor parameter characteristics for reference 95 MVA gas turbine [64].	40
7.1	investigated simulation cases, including the corresponding simulation names as well as a reference to the section where each simulation is described in detail. Furthermore, the power system model used for each simulation is presented.	45
7.2	Considered connection methods for electric ferry. Two cases are investigated where the ferry is connected fast during a ramp of one second and slow during a ramp of ten seconds respectively.	50

1

Introduction

During recent years, environmental footprints as consequences of human actions have been discovered to bring severe problems to the planet as a repercussion of increased carbon emissions. In 2020, approximately 20% of the world's total emissions originated from the sector of transportation, including public usage and different strategies of freight [2]. In order to reduce consequences of human actions and meet The Paris Agreement, rapid changes must be made to limit the impact of climate change [3]. Owing to this, efforts are being made to liquidate fossil fuels in the sector of transportation and find suitable substitutions that are more sustainable.

1.1 Background

The concept of using electricity as a replacement for the conventional combustion engine in cars and trucks is well under development and can be found to a wide extent in commercial use today [4]. The same, rapid progress, has not yet been seen in the maritime sector. In order to be in the front of the technical advancement regarding maritime electrification, Stena Line is planning to install fully electric ferries to operate the route between Gothenburg and Frederikshavn [5]. This acts as an initial step towards electrification of the maritime sector to reduce emissions.

While the concept of electric ferries may be a requirement to reach the climate goals, the implementation introduces a number of challenges. In order for the ferries to be able to travel the full distance between Gothenburg and Frederikshavn, the capacity of the batteries installed on board must be sufficient to ensure safe travels over the full distance. Furthermore, the ferries must be chargeable quickly, as they typically stay in the harbours for short periods of 60 to 90 minutes before departing once more [5]. This may become problematic due to limitations in available capacity from the power grid, as consumers have a maximum allowed instantaneous power consumption. The cost for increasing the consumers' maximum power capacity and expanding grid infrastructure to account for the increased required capacity is typically very high, while the lead time of planning through execution is long. Additionally, connecting a significant load at short times also impacts the stability of the grid. This can cause problems for the local grid regarding voltage and frequency as the instantaneous connection of a large load could act as a disturbance to the grid [6].

To tackle the presented challenges, the EU-funded project Sea Li-ion was initiated as a cooperation between DNV, BatteryLoop, Stena Recycling, Stena Rederi,

Stena Line and the ports of Gothenburg and Kiel. The target of the Sea Li-ion project is to investigate the possibility of installing Battery Energy Storage Systems (BESS) in ports, using second-life lithium-ion batteries [7]. The purpose is to boost electrification of the maritime sector by having large local BESS installed onshore in harbour areas which can be used to charge the batteries of the electric ferries. This can ensure that sufficient capacity is available for the ferries while it reduces the impact on the grid and allows faster charging than what would be possible otherwise. By using a combined feeding from the local power grid and the BESS, the connection of such a load may be achievable without causing problematic network disturbances, and without needing to significantly expand the grid capacity.

The primary functionality of the BESS as charging for electric ferries might limit its possible positive impact should the available charging capacity be high. Therefore, to further widen the applications for the BESS, investigations are made to increase the active time of the batteries without jeopardizing the charging of the electric ferries. This presents an interesting topic about how the BESS can be controlled in order to optimize its impact on the power system while still serving its primary purpose.

Further applications can potentially be to use the BESS as local grid support in order to provide stabilizing services, where the BESS can be used for peak shaving and to mitigate voltage and frequency deviations. Multiple studies show promising results regarding BESS for frequency control due to the possibility of rapidly adjusting the active power exchange to the grid [8][9]. The BESS could also be used to supply local areas in case of a total blackout where the main grid goes offline. This is referred to as island operation [10], and allows a defined part of the grid to be online in the case of failure of the main grid. This may be a very significant trait of the BESS, as it would serve as primary generation or significant support should the main power system face severe damage or outage, depending on the configuration of the islanded grid in question.

1.2 Purpose

The aim is to investigate the possible benefits of using a BESS installed in the Port of Gothenburg with a primary application of charging electric ferries to provide ancillary services for an islanded power system. The primary objective is to investigate the impact of a BESS on a local, islanded grid, primarily fed by gas turbines. Specific emphasis is placed on how the BESS can improve islanded grid operation according to the requirements of the grid code by analysing frequency and voltage behaviour.

1.3 Scope

The modelling of the BESS is limited to providing a simplified model of the battery that is sufficient for power system studies. The physical structure of the battery is

not considered. The analysis is limited to lithium-ion batteries, resulting in that the analysis may not be feasible for other technologies such as supercapacitors and hydrogen. No other alternatives of energy storage are considered. Additionally, it is assumed that the converter connecting the battery and the grid is ideal, and no considerations regarding the converter design are done.

BESS analysis behaviour is limited to the specified location of the Port of Gothenburg, and no alternative location is considered. Data regarding system characteristics is provided by parties involved in the Sea Li-ion project. Information regarding grid elements is provided by Göteborg Energi. Estimations according to public sources are made when the available data is limited or inaccessible.

As the primary target is to investigate the BESS operation for an islanded grid, no analysis is done regarding ancillary services to the main grid. For a grid-connected purpose, only a brief analysis regarding the impact of the electric ferry on the synchronous grid is conducted. This in order to investigate if the BESS serves a purpose during standard operation.

The required charging of electric ferries is to follow the schedule of the future Stena Elektra with assumed arrival and departure times. However, as this is season-dependent (peak-season and off-season), only the seasonal schedule putting most demand on the batteries will be investigated, as this would cover the feasibility for both scenarios.

1.4 Report Structure

The structure of the report is as follows. Chapter 1 serves as an introduction where general background and the target area of the report is defined. Chapter 2 and Chapter 3 introduces relevant background information serving as the base of the project. Chapter 4 covers theory connected to BESS and Chapter 5 theory behind control structures for converters. Chapter 6 presents the method of how the resulting system was implemented. In Chapter 7, the used simulation models and case studies performed are introduced. The corresponding results for the simulations presented in Chapter 7 are found in Chapter 8. Finally, Chapter 9 presents discussions regarding what has been found from the results and Chapter 10 concludes the work by summarizing the obtained results.

2

Characteristics of Electric Ferry, Harbour and Rya CHP

This chapter aims to introduce the characteristics of the future electric ferry Stena Elektra and the Port of Gothenburg. This includes the estimated energy requirements for the two as well as the daily schedule of the electric ferry. This puts the baseline requirement out of which the onshore BESS is designed. Additionally, the combined heat and power plant Rya is introduced.

2.1 Electric Ferry

The electric ferry Stena Elektra is an ongoing project with the intention of being a pioneer within maritime electrification, with a scheduled maiden voyage with passengers in 2030 [11]. Multiple projects regarding the installation of electric ferries have been conducted, and [12] presents an overview of the electric ferries that are currently in operation. As of the study in [12], it becomes clear that the capacity requirements of Stena Elektra is significantly higher than any other similar project that has been implemented. Most electric ferries are currently relatively small or travel very short distances in order to reduce the requirements of the onboard storage systems. Therefore, Stena Elektra presents a relevant research topic to investigate the feasibility of electrifying large-scale maritime vessels and pave the way for future, similar projects. An illustration of Stena Elektra is shown in Figure 2.1.



Figure 2.1: Illustration of the electric ferry Stena Elektra. Image provided by Stena Mediabank [13].

Stena Elektra is estimated to have an onboard BESS with a capacity of 70 MWh [11]. The ferry is to take tours between the harbours of Gothenburg and Frederikshavn, and the estimated energy consumption for a one-way trip is 30 MWh. This means that the onboard BESS of the electric ferry is sufficient to cover the round trip journey. Nevertheless, in order to provide sufficient margin such that the electric ferry reliably and safely reaches shore at all times, it is planned to be charged whenever berthed in a harbour. The strategy of feeding is not crucial and the ferry can be fed from the power grid if sufficient capacity and grid strength is available. However, in order to assure that the ferry can be reliably fed at all times, a BESS is planned to be installed in each harbour. The BESS dimension for the Sea Li-ion project is not yet determined. However, for this project it is dimensioned such it that ensures sufficient energy to fully charge the equivalent energy of a trip between the two harbours, regardless if the grid would be heavily loaded such that grid assistance is not possible. The required time to charge the 30 MWh for the electric ferry is estimated to be 45 minutes, resulting in a required onshore BESS power of 40 MW. The time of charging corresponds to how long the ferry is estimated to be berthed in the harbour with the availability of charging before departing once more.

The electric ferry is planned to follow two different time schedules corresponding to peak and low season, setting different requirements on how quickly and often the onshore BESS must be charged. The amount of scheduled trips during the different seasons are shown in Table 2.1. The minimum time between that a ferry departs from a harbour until the next arrives is scheduled to be approximately three hours, as two ferries are planned to be in service simultaneously. This means that the electric ferry requires the onshore BESS to be fully recharged in the corresponding time window so that it is prepared for when the next ferry arrives. The result is that the BESS must be recharged relatively quickly for the majority of the day. The only exception is the charging between the final trip of a day and the first trip of the following day, which can be conducted slowly if desired during the night. However, this must be planned corresponding to whether the BESS is to be used for ancillary services during the night or not.

Table 2.1: Seasonal schedule of electric ferry Stena Elektra. During peak season, the expected schedule is that the electric ferry travels six times per day, whereas it is only expected to travel four times per day in the low season.

	Peak season	Low season
Period	May–September	October–April
Daily trips	6	4

The charging of the electric ferry is to be conducted via an AC connection of 10 kV to the harbour substation. Therefore, only a common point of connection is installed which connects the overlying grid, the onshore BESS and the electric ferry. This is illustrated in Figure 3.3 presented in Section 3.1.2.

2.2 Harbour Loads

A harbour consists of a large variety of loads, ranging from smaller ships, harbour cranes and other equipment used for various tasks. In the Port of Gothenburg, these are supplied by Göteborg Energi through the already installed connection point to the power system. The most significant loads apart from the future Stena Elektra are ferries travelling between Gothenburg and Germany, requiring a power of approximately 1.5 MW when berthed. Harbour cranes and other machinery also correspond to high instantaneous power requirements, although during short periods of time. Regardless of this, it should be noted that the installation of Stena Elektra and other planned infrastructure requires an additional purchased connection point of feeding from the main grid. Owing to this, it is not crucial to know the exact characteristics of the harbour load profile for this purpose, as the connection point will be decoupled from the currently installed.

There are also additional loads following the installation of the electric ferry. This includes the power required for the terminal buildings and various elements around the harbour. These are kept in mind, but not modelled for simulation purposes. This is motivated behind an assumption that the loads would be relatively constant, without rapid changes in short periods of time and hence not have significant impact on the dynamic response of the system during the connection of the electric ferry. The assumed additional loads that have been neglected following the electric ferry installation are shown in Table 2.2, mainly being constituted by powering the terminal building, possible freight houses and quay lighting. The estimated significance of the load magnitude in comparison to the electric ferry is also briefly mentioned. The data is based on an available energy audit provided by BatteryLoop [14], presenting measurements from various parts of the Port of Gothenburg, such as the Germany and Denmark terminals. Assumptions are made that the corresponding loads in the new harbour section will have a similar pattern to those. Provided data indicates that the magnitude of the expected loads is small in relation to the electric ferry.

Table 2.2: Additional loads as well as power requirement in comparison to Stena Elektra as a consequence of the electric ferry installation. This includes energy to power the terminal, freight houses and quay lighting.

Load Name	Load Magnitude Compared to Stena Elektra
Terminal	Minor
Freight House	Very Minor
Quay Lighting	Very Minor

2.3 Harbour Connection to Main Grid

In order to be allowed to exchange power with the synchronous grid, a consumer must first purchase a connection point from the Distribution System Operator (DSO). The Port of Gothenburg is supplied by the DSO Göteborg Energi. Generally, it is possible to purchase a point of connection corresponding to 5, 10 or 20 MVA, as well

as different combinations of the mentioned. For the Sea Li-ion project, the contract regarding connection is not yet determined. Additionally, the planned BESS can be connected to either 130 kV or 10 kV. The two options have different cost characteristics from the DSO [15]. Generally, connecting to 130 kV has a higher corresponding fixed subscription cost, while the cost per unit energy and power is lower. Furthermore, for a 10 kV connection, the corresponding transformers connecting the BESS and the grid is owned by the DSO, while for the 130 kV connection, the corresponding customer is responsible for the transformers.

There are several options regarding the onshore BESS sizing together with different purchased connections. A high purchased power puts less stress on the BESS being able to operate each charging, as it then would act as a supplementary backup while the main grid supplies majority of the charging power during normal operation. If instead the system is built around the BESS providing charging for every time a ferry is berthed, it will cycle through the full State of Charge (SOC) range multiple times per day while potentially having less impact on the local power grid and relying less on its state. However, consequences of this is that the BESS capacity degradation will be accelerated due to the amount of SOC cycles, and that the complete discharge of the BESS makes it unable to provide support in case of unexpected grid events during certain times. Determining which strategy is the most beneficial in terms of economical and environmental aspects is a substantial task, as it depends on several future factors that can only be forecasted and estimated. This includes restructuring of the power system, generation capability, penetration of renewables and manufacturing of batteries. However, this is not included in this thesis, resulting in that the uncertainties act as the primary motivation of the chosen BESS size. As expressed in Section 2.1, the onshore BESS is in this project dimensioned such that it is able to fully charge the ferry without grid support. The benefit of this is that the relatively large BESS size can increase its possible impacts regarding alternative operation such as ancillary grid support.

2.4 Rya CHP Plant

The Combined Heat and Power (CHP) plant Rya is located close to the Port of Gothenburg. Rya is operated by Göteborg Energi and has a combined available output power of 261 MW electricity and 294 MW heat [16]. A part of the power plant consists of three gas turbines, each with an installed capacity of 45 MW [16]. The gas turbines of power plant are, in this project, considered to be suitable candidates to be used in combination with the BESS in order to operate an islanded grid around the Port of Gothenburg.

Ryaverket is a continuously developing facility, and efforts are being made by investigating alternative, more renewable fuels for the installed gas turbines in order to increase the sustainability of the power plant [17]. Furthermore, the power plant is scheduled to expand as of an environmental permit application to add a bio-steam boiler to be used together with the already installed steam turbine [18].

In order to accurately represent the dynamics of a gas turbine for simulations, multiple characteristics such as turbine compressors and temperature must be modelled [19]. Due to security reasons, information regarding this plant can not be supplied for the project as it requires security clearance. Therefore, the best estimation is given through using general templates for common gas turbine models. The most important aspects to model include the gas turbine governor and excitation system, determining how the gas turbine acts when connected to a grid.

3

Analysed Power System and Grid Requirements

The analysed power system setup is introduced, both for grid-connected and islanded configuration. The section also covers general grid requirements set by the Transmission System Operator (TSO) and DSO that are to be followed in for the customer to be allowed connection to the grid. Additionally, frequency regulating services are presented.

3.1 Overview of Investigated Power System

This section serves as an introduction to the analysed power system, where both a grid-connected model and islanded model are introduced. The considered system units are presented to indicate all elements that are included for system analysis. Furthermore, a geographical map of the harbour is included to show the location of the future electric ferry, BESS, harbour substation and Rya.

3.1.1 Geographical Orientation of Considered Grid Units

All units that are considered on a detailed level in this thesis are located in or around the Port of Gothenburg. Figure 3.1 illustrates the geographical location of the BESS, electric ferry, harbour substation and Rya. The reasoning behind the BESS placement is to minimize the distance to the electric ferry such that the transmission losses are reduced and to agree with an approximate considered location in the Sea Li-ion project. Placing the BESS as in Figure 3.1 also places it physically in between the harbour connection point and the substation. This further reduces transmission losses and material usage. An illustration of Arendal, being the focus area of the project with the future Stena Elektra berthed in the harbour is shown in Figure 3.2.

3. Analysed Power System and Grid Requirements



Figure 3.1: Geographical representation of harbour components for power system. This includes the placement of the electric ferry, BESS, Substation, Rya CHP and a simplified representation of the 10 and 130 kV cables.



Figure 3.2: Illustration of Arendal with Stena Elektra berthed in the harbour provided from [1].

3.1.2 Analysed Power System Setup

This section presents one-line representations of the power system topologies that have been investigated. Two models with similar components are introduced, being a grid-connected and islanded model respectively.

3.1.2.1 Grid-Connected System Setup

As the system investigation is conducted from the harbour point of view where the electric ferry is connected, the external grid is modelled as an aggregated representation of reality to simplify the grid behaviour. The important interfaces to model is the nearby units that are potential candidates for the islanded grid around the harbour. This includes the onshore BESS, as well as the gas turbines from Rya presented in Section 2.4. Figure 3.3 shows the connection interface between the harbour, overlying grid and onshore BESS.

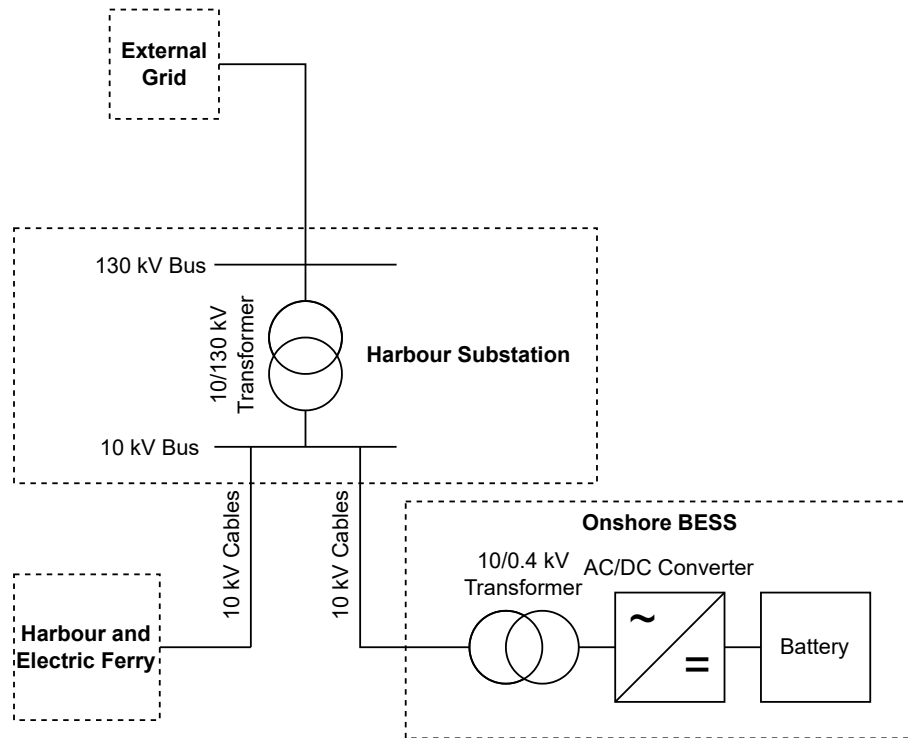


Figure 3.3: Diagram representation of investigated power system from the perspective of the harbour. The external grid is modelled as an aggregated model of the total generation and load of the synchronous grid.

3.1.2.2 Islanded System Setup

The analysed islanded system is illustrated in Figure 3.4. Elements presented in the islanded grid are the same as in the grid-connected model shown in Figure 3.3. The fundamental difference is that the grid is disconnected from the synchronous power system, removing the possibility of using the same reference unit. Therefore, either the BESS or the gas turbines in Rya must act as a generating unit that decides the system frequency. The gas turbines in Rya represent a more significant unit while the power plant has an excellent capability of being the frequency reference. Owing to this, the gas turbines are selected as a reference machine for the islanded system. Figure 3.4 shows the corresponding islanded grid setup, consisting of harbour, electric ferry, BESS, gas turbines and harbour substation.

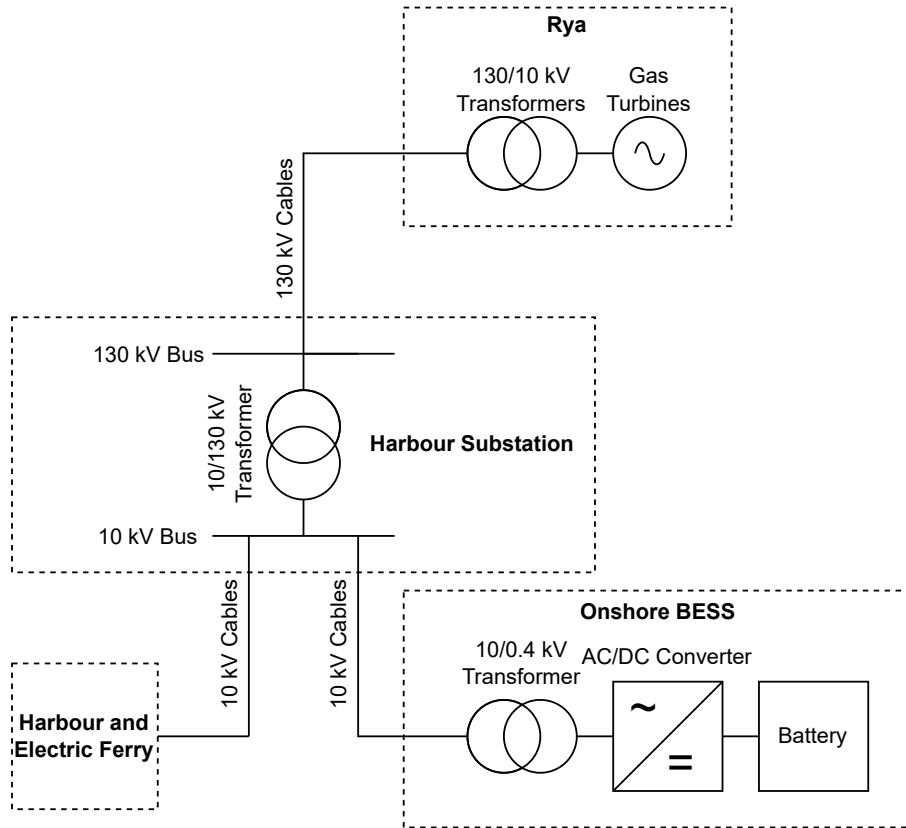


Figure 3.4: Diagram representation of investigated islanded power system from The model consists of the harbour with the electric ferry, the BESS, gas turbines in Rya as well as the harbour substation interface.

3.2 Grid Requirements

An electrical power system is a sensitive infrastructure. Therefore, requirements are set to assure that a grid can operate safely without interruptions. Some of these include voltage magnitude guidelines, frequency requirements and requirements on generating units. This section aims to introduce important guidelines that should always be followed that are provided by the TSO and DSO.

3.2.1 Voltage Requirements

In order to preserve the integrity of the power system, certain demands are specified on voltage magnitudes by the TSO and DSO. The local DSO Göteborg Energi follows the guidelines presented in EIFS 2013:1 in order to assure that system voltages are kept within acceptable limits during certain time periods [20]. One requirement is that all voltage measurements performed in ten minute intervals should have a magnitude within the window of 90% to 110% of the nominal system voltage. Furthermore, the customer is allowed to have a 4% voltage drop within the corresponding installation to account for transmission losses in low voltage cables and other grid elements.

3.2.2 Frequency Requirements

A general power system is sensitive to frequency deviations from that of the nominal. This is due to that many generating units as well as various loads require a certain frequency in order to function properly. Therefore, requirements on frequency are set to assure that a power grid remains stable. For the Nordic power system, a general requirement is that the frequency should be kept above 49 Hz during a severe disturbance to assure that the system remains intact [21]. If the frequency decreases below 49 Hz, load shedding and other actions can be taken in order to preserve system stability. This is undesired, and it is of high importance to keep the frequency close to that of the nominal. The frequency range for standard operation is specified to the frequency window of 49.9–50.1 Hz.

It is common that generating units have a characteristic that react with a response in power output to frequency deviations, should the grid frequency differ from that of the nominal frequency. The frequency in the power grid is changing continuously, resulting in that a direct frequency control could create a shaking generation from droop-controlled units. Therefore, a deadband of 100 mHz is required, both above and below the nominal frequency [22] when providing frequency support for disturbances to the main grid. The purpose of this is to create a regulation that can assist during abnormal conditions, while it is idle during standard operation close to nominal system frequency. If a deadband for the droop-base control is not introduced, there is a possibility to have a shaking generation regulation around nominal frequency, which could worsen the system behaviour during steady-state operation while it also creates additional stress on generating units. The described characteristic is shown in Figure 3.5, which shows the change in active power output ΔP with respect to the system frequency. If the measured frequency deviates more than the set deadband from the nominal system frequency f_{nom} , the corresponding unit will increase or decrease its active power output as a linear function of the frequency deviation, depending on if the frequency is below or above that of the nominal.

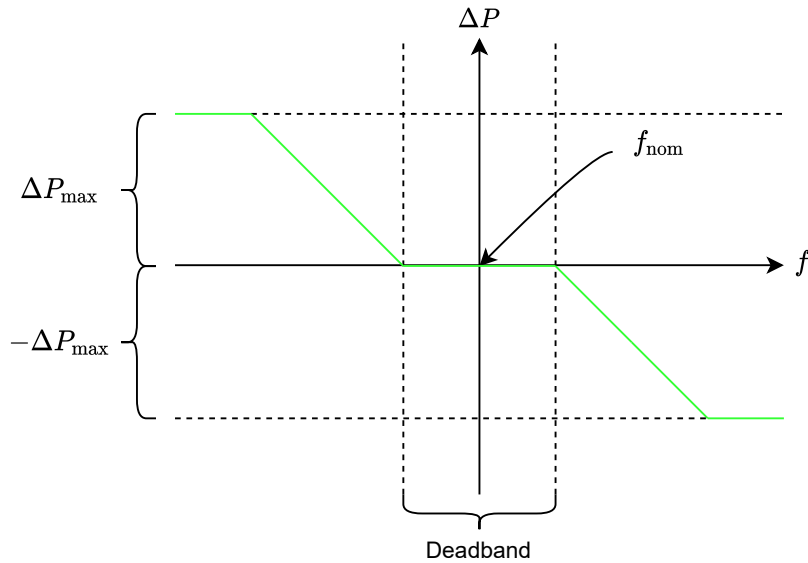


Figure 3.5: Generation unit characteristic for active power output versus frequency. If the measured frequency is within the deadband, the corresponding change in active power output ΔP is zero. When the frequency is outside the deadband, the active power output is a linear function of the frequency deviation. The nominal system frequency is marked and expressed as f_{nom} .

The synchronous system frequency is continuously measured and the Swedish TSO Svenska Kraftnät (SVK) publicly offers access to the frequency statistics [23]. Figure 3.6 shows the system frequency for 2022–03–01 between the time of 06:00–07:00 to show frequency variations during an arbitrary day. The allowed frequency span is marked, and the measurements indicate that the frequency normally is kept within 100 mHz from the nominal frequency.

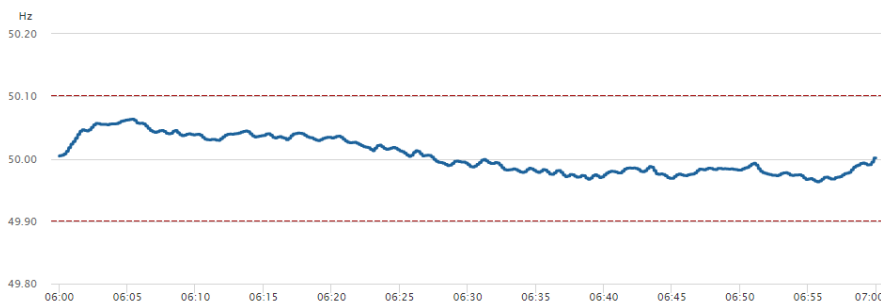


Figure 3.6: Measured system frequency on 2022–03–01 during the time of 06:00–07:00, as well as indications of normal allowed frequency deviations from the nominal [23]. Frequency data on the official SVK website is provided by Statnett.

3.2.3 Generator Requirements

In order to be allowed to connect a generating unit to the grid, specific requirements must be met [22]. Firstly, the active power setpoint must be changeable with re-

gards to what is instructed by the grid operator. A general requirement is that the active power output of a generating unit should be adjustable such that it can be changed from maximum generation to half within a time period of one minute [22]. There are also specific requirements regarding change in active power depending on the type of generation unit, as different technologies act substantially differently. This includes that the generating unit should be able to manage specific steps in active power over a certain time period. For this purpose, BESS provide an excellent opportunity due to its possibility to quickly change its corresponding active power exchange with the respective grid. This is because the BESS does not have any rotating mass compared to many other commonly used generating technologies, allowing more rapid changes due to the reduced mechanical constraints.

There are also requirements regarding the operation of generators within different frequency ranges. For European grids, certain frequency requirements are entirely regulated by the European Network of Transmission System Operators for Electricity (ENTSO-E) [24]. Additionally, the basic guidelines are not strictly the same for all grid regions. For the Nordic synchronous system, generating units are required to continuously operate within the frequency region of 49–51 Hz. Outside of this frequency window, units must only be able to operate for a defined time interval. The set requirements for the Nordics is shown in Table 3.1.

Table 3.1: Required operation times for generating units connected to the Nordic synchronous system [24]. The frequency range of 49.0 – 51.0 Hz is considered the norm where continuous operation is expected. Outside of this frequency range, generating units are only required to properly function for a limited time period.

Frequency Range	Time period for operation
47.5 Hz – 48.5 Hz	30 minutes
48.5 Hz – 49.0 Hz	To be defined by each TSO, but not less than 30 minutes
49.0 Hz – 51.0 Hz	Unlimited
51.0 Hz – 51.5 Hz	30 minutes

3.3 Frequency Regulating Services

In order to maintain a system frequency that is close to that of the nominal so that system stability is assured during normal operation, generating units can be used to change their corresponding output power to balance the power system. This is referred to Frequency Containment Reserve (FCR), where units have an active power versus frequency characteristic similar to what is shown in Figure 3.5 presented in Section 3.2.2. Units providing this service are directly selling regulating services to the power system, for which the corresponding owner is awarded. The FCR-market is divided into two sections being Frequency Containment Reserve for Normal Operation (FCR-N) [25] and Frequency Containment Reserve for Disturbances (FCR-D) [26][27]. The award for providing these services is determined through bidding that occurs one and two days prior to when the unit in question is to provide the agreed upon service.

4

Battery Energy Storage Systems

This chapter serves as an introduction to BESS. It covers how BESS can be applied for power system applications and the general structure of a grid-connected BESS. Additionally, strategies of modelling batteries for simulation purposes are presented, as well as important battery properties.

4.1 BESS for Power System Applications

Large scale energy storage systems have become attractive for power system applications due to several reasons. BESS offer the possibility to quickly change its active power exchange with the grid that it is connected to. Therefore, the BESS can be used efficiently should the grid face loss of generation or see significant increases in load. Furthermore, BESS can be controlled in order to act as a reference machine for a grid and hence decide the system frequency. This becomes an important trait, as it enhances the possibility of running small, islanded power systems without conventional synchronous machines should the main grid be out of service, which for instance may occur due to generator tripping or damaged infrastructure. The application of BESS is further expanded by the ongoing trend of replacing conventional generation units using fossil fuels to renewable energy, mainly wind and solar [28]. This because of two main aspects, the first being that the transition to renewables results in a reduced overall inertia of the power system, making it less redundant in case of large load connections or generation losses [29]. For this purpose, BESS can provide frequency support and quickly inject active power to counteract severe frequency deviations and potential blackouts. The second aspect is that renewable energy lacks the possibility of providing a sustained, reliable power output throughout the day, as it depends on solar radiation and the wind. Therefore, BESS provide an excellent possibility of being charged during times of high production, to be discharged in order to compensate at times where production is low. This enhances the motivation behind the BESS as the trending direction of generation technologies may require significant storage capability in order to be feasible.

The major consequence of BESS for different applications, not only power systems, is the manufacturing process of battery technologies. This includes that of lithium-ion batteries as well as other popular battery chemistries [30]. Owing to this, the investigation of alternative methods of production is a relevant topic, attracting a significant amount of market participants. An example for this is the ongoing planning for a large factory for battery manufacturing in Gothenburg by Northvolt

and Volvo Cars [31]. These projects become significant factors for the installation of large BESS and may elevate the motivation behind investing in storage systems.

4.2 BESS Structure

A BESS consists of multiple components in order to properly function in symbiosis with a corresponding power system. The main electrical structure is constituted by a battery and a DC/AC converter that acts as the interface between the battery and corresponding connection point. However, in order to manipulate the BESS behaviour such that it can be controlled to act depending on the grid circumstances, control strategies must be employed. This includes a controller for the converter, modifying the output of the converter. Additionally, a Battery Management System (BMS) is crucial in order to ensure that the battery operates safely and efficiently to mitigate the possibility of battery destruction and lifetime reduction [32]. Battery protection is not included in this project, resulting in that the BMS has been neglected. The general structure of a grid-connected BESS is shown in Figure 4.1.

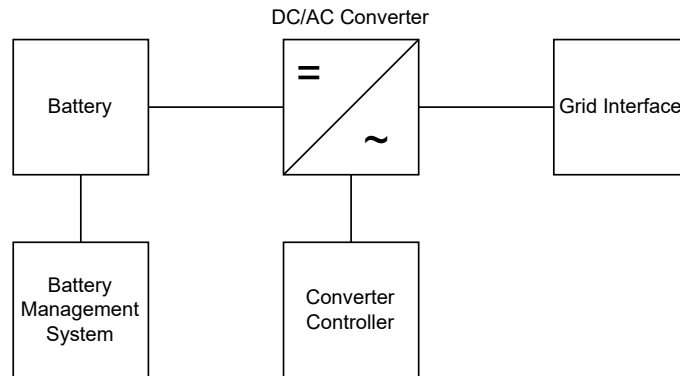


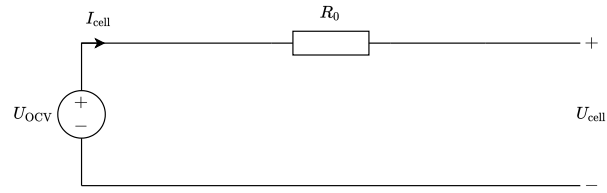
Figure 4.1: Generic structure of a grid-connected BESS. The primary elements are the battery, converter, BMS and converter controller. The BMS monitors the corresponding battery packs within the battery to ensure safe and reliable operation, while the converter controller decides the BESS power exchange with the corresponding power system.

4.3 Electrical Modelling of Lithium-Ion Batteries

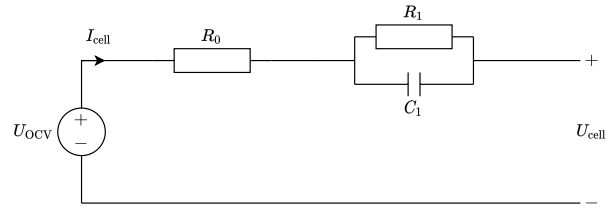
This section aims to introduce the concept of modelling for lithium-ion batteries for a power system application. Different approaches are mentioned, and the preferred for the purpose of this project is motivated. Furthermore, some of the most important parameters to consider when modelling lithium-ion batteries are highlighted. This includes the impact of temperature, state of charge and capacity degradation.

4.3.1 Equivalent Circuit Model Representation

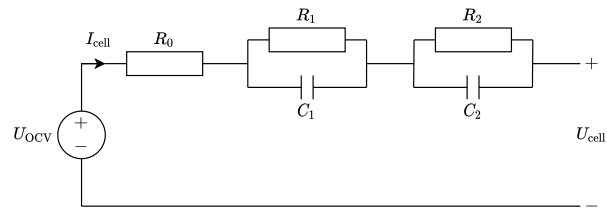
As the dynamics of batteries are based on chemical reactions and processes, the behaviour of battery cells depends on several physical properties that are constantly changing with regards to the structure of the battery as well as the surrounding environment. It is possible to derive and use electrochemical models to quite accurately represent the physical behaviour of battery cells [33], based on physical properties and chemical reactions. However, these models generally require significant computational power and are difficult to accurately parameterize. An alternative is to use an Equivalent Circuit Model (ECM) [34]. The purpose of this is to derive battery models that can be represented electrically through passive electrical components, and hence be more suitable for studies on power system level. There are several methods to represent battery behaviour through ECMs, depending on the required accuracy and the characteristics of the battery [34]. The general modeling is based on a simple structure with a voltage source representing the Open-Circuit Voltage (OCV) connected to impedance links. Figure 4.2 shows example structures of three different ECMs with gradually increasing complexity and accuracy, where U_{OCV} is the open-circuit voltage, R_0 represents the ohmic resistance of the battery, R_1 and R_2 the polarization resistances and C_1 and C_2 the polarization capacitances. Polarization is a complex dynamic of batteries that includes multiple processes that occur [35]. This includes battery properties such as contact problems between solid phases, mass transport limitations and that some chemical reactions occur slowly [35]. For studies where it is important to very accurately represent the battery dynamics, several RC-links of polarization impedance representations are used, where each link is tuned differently to correspond to its own dynamic response.



(a) Simple model, no polarization.



(b) First-order model.



(c) Second-order model.

Figure 4.2: Equivalent circuit models of lithium-ion batteries with increasing complexity. The most trivial model (Figure 4.2(a)) consists of an OCV in series with a pure resistance to account for the internal voltage drop of the battery.

Higher order models (Figure 4.2(b) and Figure 4.2(c)) include parallel RC branches to represent polarization processes and hence present a more dynamically accurate battery model.

The parameters of an ECM are commonly obtained through fitting according to experimental testing on battery cells and can represent battery behaviour without major error [36]. A drawback of this approach is that the individual impact of effects on battery modelling can not be directly analysed to the same degree as in electrochemical models unless targeted specified measurements are performed, which in turn include several uncertainties. However, it can simulate battery behaviour during certain conditions with good precision and fast computation. This becomes important when the battery is to be simulated for grid applications, where the computational speed must be sufficiently fast. Furthermore, for power system applications, it is important to be able to accurately determine the terminal voltage, battery current, output power and SOC. This in turn to correctly estimate the state

of the battery such that it operates within its specified allowed limits.

In order to estimate the terminal voltage at a given SOC, the corresponding transfer function between terminal voltage and current can be used. For an arbitrary ECM of order m , the transfer function is given according to Equation (4.1). The transfer function illustrates the internal voltage drop of the battery from OCV to terminal voltage, where R_0 , R_m and C_m are treated as functions of dynamic properties such as SOC and temperature.

$$U_{\text{cell}} = U_{\text{OCV}} - i_{\text{cell}} \left(R_0 + \sum_{n=1}^m \frac{R_m}{sC_m R_m + 1} \right) \quad (4.1)$$

4.3.2 Temperature

Temperature is an important parameter to consider when determining the performance for a lithium-ion battery and has major effects on battery behaviour. Temperatures below zero degrees celsius show a significant increase in internal resistance and should hence be avoided [37]. The internal resistance generally always increases with decreasing temperature. However, on the other hand, operation at high temperatures can cause thermal runaway and direct destruction of the battery cell [37], resulting in that Li-ion batteries require accurate strategies for temperature prediction and control. The temperature also directly affects the available capacity of a battery cell and very low temperatures can ultimately cause major losses of capacity [38]. Nevertheless, one can decide to model batteries under the assumption of a constant operating temperature in order to neglect this effect and make the dynamic modelling significantly less complicated. This is generally a fair assumption as long as the charging current is limited, and the battery stored within a confined space with proper cooling such that the temperature can be controlled to what is desired. For fast charging, temperature rise may be difficult to mitigate due to heating from high currents. However, it should be noted, as previously highlighted, that the internal resistance is inversely proportional to the temperature. This results in that a temperature rise may not be that detrimental to the impedance as long as a thermal runaway is not triggered. Nevertheless, temperature also has a significant impact on other important properties, which is brought to attention in Section 4.3.4.

4.3.3 State of Charge

The SOC represents a measure of the remaining capacity within a battery in comparison to the nominal capacity when the battery is fully charged. It is a direct indication of how an operation depletes the charge of a battery. The OCV of a lithium-ion battery is directly influenced by the SOC at a given moment, and increases with the SOC [39]. This relation is obtained by performing experimental measurements of the cell of interest, often in combination with tests for parameter estimation as mentioned in Section 4.3.1. This can then be used during the operation of the battery if the SOC is tracked in order to estimate the OCV. The measurement of SOC can be done in multiple ways, where a commonly used method is Coulomb Counting [39]. The method is based on measuring the current and integrating it in

order to measure the charge throughput and hence the change in SOC as

$$\Delta SOC = \frac{1}{Q_{\text{nom}}} \int_{t_1}^{t_2} i(t) dt, \quad (4.2)$$

where ΔSOC is the change in SOC, Q_{nom} is the nominal capacity of the battery, t_1 and t_2 the starting and ending time of charge or discharge. The main drawback of this is that an initial SOC must be known in order for the measurement to be reliable. If there is an initial error, the integration continuously increases the error which can eventually lead to severe miss-estimations of the SOC. This would then further follow that the OCV of the battery is also poorly estimated.

The operation of lithium-ion batteries is highly connected to the SOC at a given time as the battery chemistry is continuously changing. The equivalent battery impedance is greatly affected by the SOC and therefore also the terminal voltage and current for a specific operation. The SOC at which a battery is stored has a significant impact on its lifetime [40]. Storing a lithium-ion battery at high SOC can enhance various ageing effects such as electrolyte decomposition and porosity [41]. Furthermore, charging a lithium-ion battery to high SOC with a high current can cause direct destruction of battery cells as it can result in lithium plating [42], forming dendrites that pierce the structure of the battery.

4.3.4 Capacity and Power Fade

The lifetime of a lithium-ion battery is commonly defined as the time from beginning of life until the battery has reached a 20% capacity fade [43]. This means that capacity degradation-rate must be monitored and preferably reduced as much as possible without compromising the possibility of the battery to perform its assigned tasks, in order to maximize the lifetime. The Depth of Discharge (DoD), being a measure of how much of the SOC range that is used for each discharge or charge cycle directly influences the number of cycles that can be expected during the lifetime of a battery [43].

Many aforementioned parameters have significant impact on the lifetime of a battery cell. The primary parameters that impact battery lifetime are depth of discharge, discharge rate and temperature [44]. In [45] it is mentioned that the capacity of a lithium-ion battery degrades if the temperature is beyond 50° C, no matter of the discharge rate or cell chemistry. Furthermore, storing a battery at a high SOC can accelerate capacity fade [46]. All of these factors must hence be considered when designing a BESS in order to maximize lifetime and overall performance, such that the possible economical and environmental profits can be optimized.

4.4 Impacts of Second-Life Batteries

The target of the Sea Li-ion project is to use second-life lithium ion batteries to design the onshore BESS. Following from this are environmental benefits compared

to using new batteries, as the primary battery manufacturing process is unrelated to the BESS. Additionally, the current, rapid trend of electric vehicles presents a significant source of second-life batteries [47]. Due to the high required instantaneous powers for sufficient acceleration in an electric vehicle, as well as the limited amount of space and weight for batteries, a battery for this purpose has stricter requirements to operate adequately. For grid applications, this issue is generally not a problem as a BESS for this purpose can be significantly larger in space. This results in an opportunity of combining the two applications to make more use of each produced battery cell, elevating both environmental and economical aspects significantly.

Considering the reduced relative battery performance with that of beginning of life, a consequence of using second-life batteries is that it introduces new challenges. In [48], it is found that batteries with a high internal impedance may introduce difficulties, should they be used during second-life for demanding applications. Another critical task is the difficulty of estimating when the second-life batteries can no longer be used, as the corresponding battery degradation is currently relatively unknown [49]. This may prove to be a difficult task, considering that a degradation that is more rapid than anticipated can lead to battery failure before the estimated end of life for secondary use. Additionally, [49], mentions the importance of monitoring how batteries are used in their first life, as many cells may be insufficient to fulfill the requirements of second-life.

5

Converters and Control Concepts

The most common control structures of converters and their fundamental operating principles are presented. The main difference between grid-forming and grid-following converter structures are assessed. Furthermore, control-concepts used for these converters are introduced. This serves as background theory for the implemented converter control strategy, and an introduction to concepts that have been investigated.

5.1 Converter Control Structures

The concepts of grid-following and grid-forming converters are discussed. The operational control structures and differences are introduced. Furthermore, the advantage of grid-forming control is highlighted and when it may be preferred to use.

5.1.1 Grid-Following Converter

Grid-following converters are often found as interfaces between generating units and power systems. Commonly, these converters are fed with references of active and reactive power in order to set the output voltage [50], and hence control the injected current [51]. This is often done by the implementation of power controllers cascaded with a current controller. However, in order to perform this action, knowledge of the phase angle at the PCC is required in order to have the converter synchronized with the grid. This is commonly achieved by implementing a phase-locked-loop [52].

5.1.2 Grid-Forming Converter

Grid-forming converters can conceptually be seen to have similar tasks as grid-following converters, consisting of controlling the output active and reactive power at the PCC (or by other words the power exchange between the grid and the converter). However, as opposed to the operation of the grid-following converters, the grid-forming converter is designed to control the voltage at the PCC, both in amplitude and phase [51], rather than the injected current. As a result, this converter does not strictly require knowledge of the phase angle at the PCC, and can during no-load operation act as a reference setpoint for the grid it is connected to [53]. This becomes an important trait for grid-forming control, as it allows the converter to be used efficiently as a reference machine for isolated grids during island operation. This in turn results in the possibility of using the BESS to black-start islanded

power systems, and to use it efficiently in combination with other generating units that require a reference machine. Additionally, grid-forming converters can perform better in weak grids and allow the possibility to provide virtual inertia to reduce the Rate-of-Change-of-Frequency (RoCoF) following a grid disturbance.

The control of grid-forming converters can be designed by multiple methods such as Power Synchronization Control, Virtual Synchronous Machines, Synchroverters or Virtual Oscillators [51], where the characteristics of the control are different. Often, the different controls are designed to perform certain operations and have non-optimized behaviour for other aspects. The control concepts considered in this project are presented in Section 5.2.

5.2 Converter Control Concepts

This subsection aims to introduce concepts for controlling grid-forming converters. The implementations of power synchronization control and virtual synchronous machines are presented, as well as the control structure used in this project.

5.2.1 System Model for Control Derivation

The model used to derive control system approaches for the grid-forming converter is shown in Figure 5.1. It consists of the BESS, modelled as a voltage source to represent the battery behind an ideal converter. Furthermore, an impedance Z_f is added to represent the converter filter, being a series RL-impedance. Additionally, the overlying grid is modelled as an ideal voltage source behind a series RL-impedance Z_g , to represent the strength of the grid. For a strong grid, the equivalent grid impedance Z_g is low whereas for a weak grid, the corresponding impedance is higher.

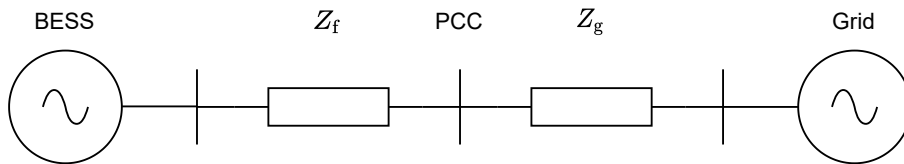


Figure 5.1: Simplified network model used for derivation of control concepts for grid-forming converter. The model consists of a voltage source representing the BESS with a series RL-filter Z_f as well as the overlying grid, together with the grid equivalent impedance Z_g .

5.2.2 Power Synchronization Control

A widely known and used concept in power system analysis is the theory behind how active and reactive power is connected to the angle difference between buses and voltage magnitudes [54]. The active power transfer between two points is strongly connected to the difference in phase angle, while the reactive power transfer is strongly

connected to the difference in voltage magnitudes. The active power exchange between two arbitrary buses can be expressed as

$$P = \frac{V_s V_r}{X} \sin \delta, \quad (5.1)$$

where V_s is the voltage magnitude from the sending bus, V_r the voltage magnitude at the receiving bus, X the total reactance between the buses and δ the difference in voltage angle. Power Synchronization Control (PSC) is a method of synchronization by using an active power controller. The active power controller ensures that the system approaches the reference active power by changing the reference voltages used for the Pulse Width Modulation (PWM) pattern of the converter. A method to synchronize the active power to the reference is presented in [54], where the basic system block diagram is shown in Figure 5.2 and the adopted control law is given as

$$\frac{d\Delta\theta}{dt} = \omega_1 + K_p(P^* - P), \quad (5.2)$$

where $\frac{d\Delta\theta}{dt}$ is the change in angle with respect to time, ω_1 the nominal system frequency, K_p the active power controller proportional gain, P^* the reference active power and P the measured active power transfer.

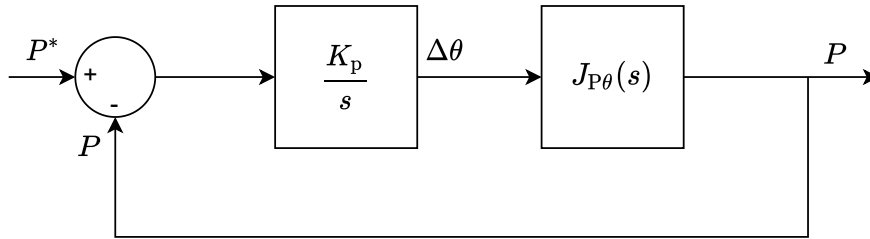


Figure 5.2: Block diagram of basic PSC structure, consisting of proportional control parameter K_p and the corresponding transfer function between θ and P , expressed as $J_{P\theta}(s)$ [54].

Furthermore, [55] suggests adding an active damping term to mitigate oscillations around the power reference setpoint. This is done by feeding the measured dq-frame current through a high-pass filter as well as a gain block and subtracting it from the nominal voltage magnitude in the dq-frame. The resulting inner control structure of this controller is shown in Figure 5.3.

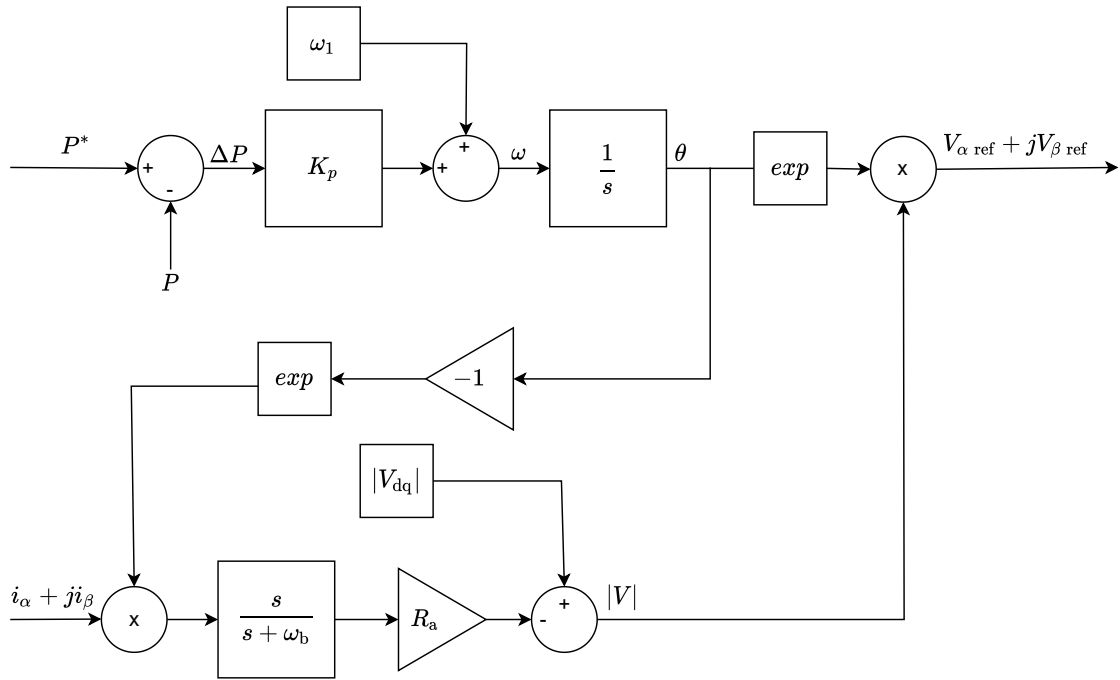


Figure 5.3: Block diagram of PSC control structure with active damping from measured current from [55].

The tuning of K_p is suggested from [55] to be set according to

$$K_p = \frac{\omega_1 R_a}{\kappa V^2}, \quad (5.3)$$

where R_a is the introduced active damping resistance, κ a constant depending on which transformation method between $abc/\alpha\beta$ -frame that has been used ($\kappa = 1$ for power invariant transformation, which has been used for this project) and V the nominal voltage magnitude of the system in dq-frame. The active damping resistance R_a originates from that [55] recommends subtracting a high-pass filtering from the voltage magnitude V , which is governed by the transfer function of

$$H_a(s) = R_a \frac{s}{s + \omega_b}, \quad (5.4)$$

where ω_b the filter bandwidth, typically selected depending on the nominal angular frequency as

$$\omega_b \approx 0.1\omega_1. \quad (5.5)$$

The high-pass filter is used in order to reduce oscillations of the system by using the measured current, which otherwise can be prone to significant oscillations in output active power P , resulting in a less stable system operation.

5.2.3 Virtual Synchronous Machine

One disadvantage with the active power control presented in Section 5.2.2 is that it does not allow the converter to provide virtual inertia to the system. Inertia is an important characteristic of power systems which is directly connected to the

robustness of the system. The transition from large rotating machines to converter-based generation directly reduces the direct inertia of a power system. This may result in systems where a high RoCoF is possible, which raises concerns regarding system stability. Therefore, it is desired to design converter control interfaces such that virtual inertia [56] can be achieved. A well-researched and relatively simple way of implementing this is to mimic the behaviour of synchronous machines by Virtual Synchronous Machines (VSM) [57]. Synchronous machines are typically described through the swing equation, and [58] shows the conventional VSM control structure as

$$\theta = \frac{1}{s}\omega_{\text{conv}} = \frac{1}{s} \left[\omega_1 + \frac{1}{sM + K_D}(P^* - P) \right], \quad (5.6)$$

where θ is the angle of the voltage at the converter, M the virtual inertia scaled to ω_1 , K_D the virtual mechanical damping constant and P^* the reference active power. Additionally, M is found from the virtual inertia constant H and ω_1 through

$$M = 2H\omega_1. \quad (5.7)$$

Comparing Equation (5.6) with the transfer function presented in Equation (5.2), it can be seen that the active power control gain K_p can be replaced by the swing equation as

$$K_p = \frac{1}{sM + K_D}. \quad (5.8)$$

The new closed-loop system of the active power-control can then be expressed by the block diagram shown in Figure 5.4, where the variables V_c , V_g and X_f represent the grid voltage magnitude, converter voltage magnitude and converter filter reactance.

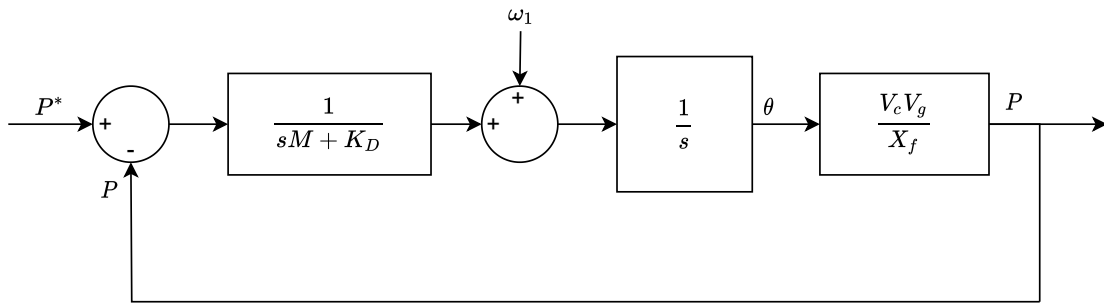


Figure 5.4: Block diagram for PSC with K_p replaced by swing equation. The system transfer function between θ and P is expressed as $\frac{V_c V_g}{X_f}$.

The closed-loop transfer function $G_{\text{cl VSM}}(s)$ for the VSM control structure in Figure 5.4 is given by

$$G_{\text{cl VSM}}(s) = \frac{\frac{1}{sM + K_D} \frac{1}{s} \frac{V_c V_g}{X_f}}{\frac{1}{sM + K_D} \frac{1}{s} \frac{V_c V_g}{X_f} + 1}. \quad (5.9)$$

Resulting is that the expression of $G_{\text{cl VSM}}(s)$ corresponds to a second-order transfer function $H(s)$ with the characteristic of

$$H(s) = \frac{\omega_n^2}{s^2 + 2\zeta\omega_n s + \omega_n^2}, \quad (5.10)$$

where ω_n is the natural angular frequency and ζ the damping ratio. By comparing $G_{\text{cl VSM}}(s)$ with $H(s)$ the representation of each term can be assessed, and the control structure can be tuned so that the desired natural angular frequency and damping can be obtained.

5.2.4 Active Power Control with PI-Controller

A significant drawback with using the VSM from Section 5.2.3 for the active power control is that the control becomes incorrect should the grid frequency deviate from the nominal frequency, according to the damping term K_D . Resulting is a steady-state error between the output power of the converter and the set reference power. To mitigate this, the implemented swing equation can be replaced by a PI-controller that is able to force the steady-state error in power to zero. This becomes an important trait, as the system frequency more often than not deviates from the exact nominal frequency, ultimately resulting in that the PI-controller is arguably the best choice for the converter control for this application. The block diagram for the PSC with a PI-controller is shown in Figure 5.5, where K_p represents the proportional gain and K_i the integral gain. A feedback of the power P is implemented through a gain R_{al} in order to implement active damping. This is done in order to reduce overshoots in active power output when a new reference power setpoint is given.

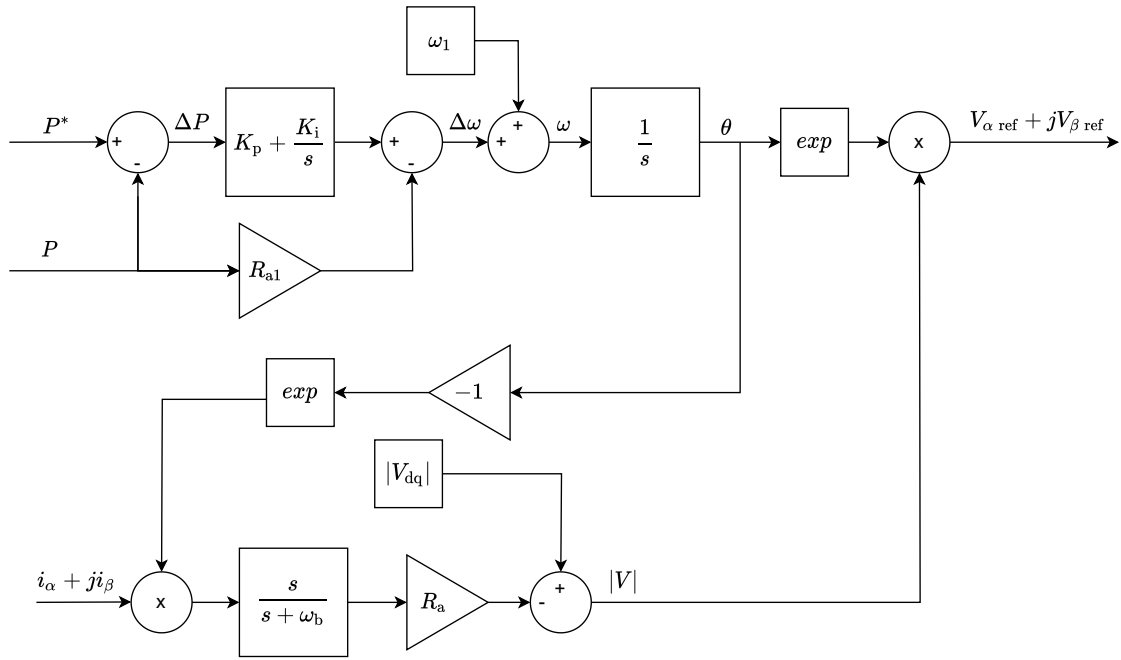


Figure 5.5: Block diagram of active power controller, constituted by a PI-controller that takes measured active power and active power reference as input. A damping term R_{a1} is added to reduce overshoots in active power output when a reference power is given to the control system.

The tuning of K_p , K_i and R_{a1} are attempted through two strategies, where the first strategy is presented in [59] and [60], whereas the second approach is based on deriving the closed-loop transfer function. The purpose of both strategies is to tune the parameters such that the pole of the closed-loop transfer function is cancelled. The effect of this is to cancel overshoots in the active power generated, as significant overshoots are not allowed and may damage equipment. The block diagram of this system representation is shown in Figure 5.6.

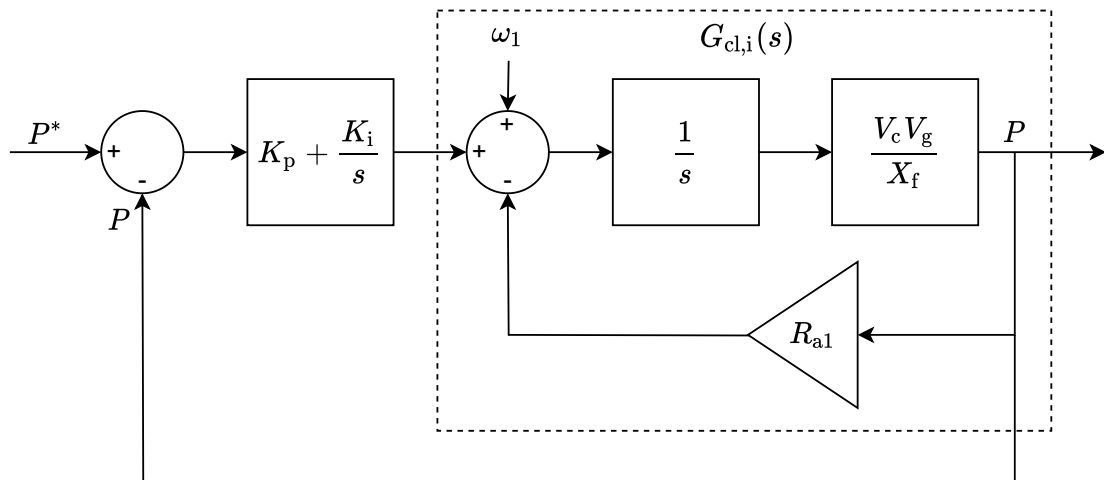


Figure 5.6: Block diagram of active power control with PI-controller.

The closed-loop transfer function of this system configuration can be derived by the same strategy as applied in Section 5.2.3. For this case, the transfer function includes an inner closed-loop transfer function $G_{\text{cl},i}(s)$ that can be expressed as

$$G_{\text{cl},i}(s) = \frac{\frac{1}{s} \frac{V_c V_g}{X_f}}{\frac{1}{s} \frac{V_c V_g}{X_f} R_{a1} + 1}. \quad (5.11)$$

Simplifying the expression and introducing $K' = \frac{V_c V_g}{X_f}$ yields the expression for the inner closed-loop transfer function as

$$G_{\text{cl},i}(s) = \frac{1}{sK' + R_{a1}}. \quad (5.12)$$

Using the expression for $G_{\text{cl},i}(s)$ from Equation (5.12), the full closed-loop transfer function is given as

$$G_{\text{cl},\text{PI}}(s) = \frac{K_p s + K_i}{s^2 K' + s(R_{a1} + K_p) + K_i}. \quad (5.13)$$

This can be seen as a generic transfer function $G(s)$ with the bandwidth α with the corresponding shape of

$$G(s) = \frac{\alpha s + \alpha^2}{s^2 + 2\alpha s + \alpha^2}. \quad (5.14)$$

In order to remove overshoots in the system response, the pole of the closed-loop transfer function should be eliminated. By setting $G_{\text{cl},\text{PI}}(s) = G(s)$, the tuning for the corresponding PI-controller in the control-loop can be found as

$$\alpha = \sqrt{\frac{P_{\text{max}}}{M}} \quad (5.15)$$

$$K_i = \frac{\alpha^2}{P_{\text{max}}} \quad (5.16)$$

$$K_p = \frac{\alpha}{P_{\text{max}}} \quad (5.17)$$

$$R_{a1} = K_p, \quad (5.18)$$

where α is the bandwidth of the controller, P_{max} the maximum power transfer between the converter terminal and the PCC as $P_{\text{max}} = \frac{V_c V_g}{X_f}$ and M the virtual inertia scaled to ω_1 . The controller takes input signals corresponding to the measured active power P at the PCC, the reference power P^* and the $\alpha\beta$ -frame currents $i_\alpha + j i_\beta$. The powers are fed through a PI-controller which gives an output that corresponds to a differential angular frequency, which is then subtracted from the nominal angular frequency of the system. Integrating the angular frequency gives the resulting phase angle. The required voltage magnitude together with the phase angle yields the corresponding reference voltages in $\alpha\beta$ -frame.

5.2.5 Voltage Control

In order to prevent the voltage at the PCC from deviating significantly from the nominal value, a voltage controller can be implemented. The controller can be

designed as a pure integrating controller as suggested in [60]. The block diagram of the voltage controller is shown in Figure 5.7, where $|V_{dq}|$ is the measured voltage magnitude in dq-frame, V_{nom} the nominal voltage, $|V_{dq}^*|$ the resulting controlled voltage and K_{ivc} the integrator gain.

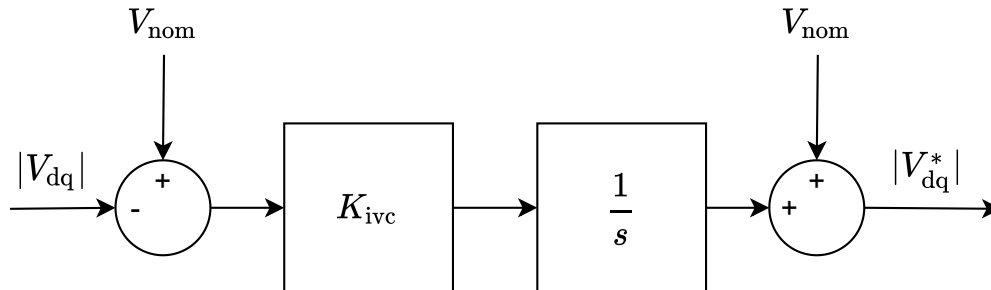


Figure 5.7: Block diagram of voltage controller that keeps the voltage at the PCC close to the nominal voltage. The controller compares the measured PCC voltage magnitude in dq-frame with the nominal voltage magnitude.

The integrator gain is tuned according to [60] as

$$K_{ivc} = \frac{\alpha_{vc}(X_f + X_g)}{X_g}, \quad (5.19)$$

where α_{vc} is the bandwidth of the voltage controller, X_f the filter reactance of the converter and X_g the reactance of the grid. The voltage controller can be connected in cascade with the active power controller presented in 5.2.4. Therefore, [60] suggests that the bandwidth of the voltage controller is set greater than that of the active power controller.

5.2.6 Frequency Control

A frequency controller can be designed as a simple proportional controller that takes the measured frequency as input and subtracts it from the nominal frequency. The result is fed through a proportional gain that scales the frequency deviation to represent a reference power that should be fed to the system. The block diagram of such a frequency controller is shown in Figure 5.8. This creates a droop characteristic where the proportional frequency controller gain $K_{p \text{ freq}}$ represents the droop setting of the BESS.

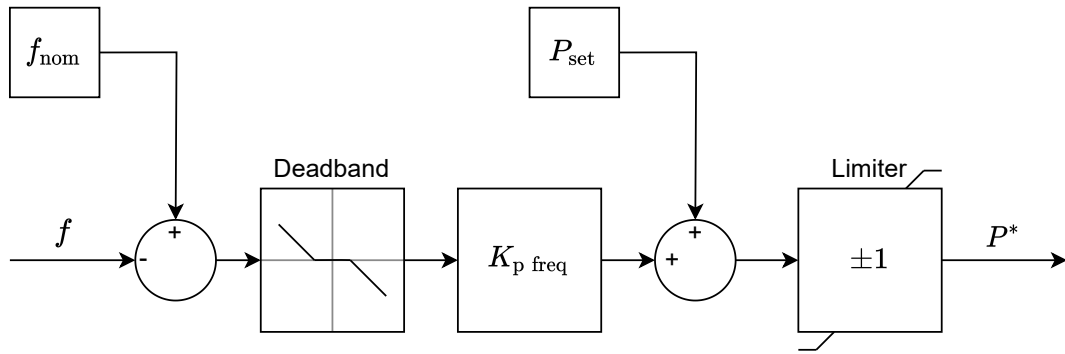


Figure 5.8: Block diagram of frequency controller to provide reference active power setpoint for BESS control system. The control system takes the measured system frequency and compares it to the reference frequency to set the corresponding reference active power.

This topology of frequency controller will cause the BESS to charge or discharge whenever the system frequency deviates more than the defined deadband from the nominal frequency. This may not be desired, as it would result in that the BESS can discharge quickly as it could be in continuous operation if the load increases. To mitigate this, an alternative is to design the frequency controller such that the BESS assists the grid with active power should there be an event that changes the system frequency, but then slowly reduce its active power output to zero. This can be done by adding a high pass filter to the frequency controller, where the corresponding time constant determines the time for the BESS output power to reach zero. The adjusted frequency controller can be seen in Figure 5.9. The result of this strategy is that the initial frequency response increases as the BESS activates, but the steady-state frequency will eventually converge to the same as without the BESS.

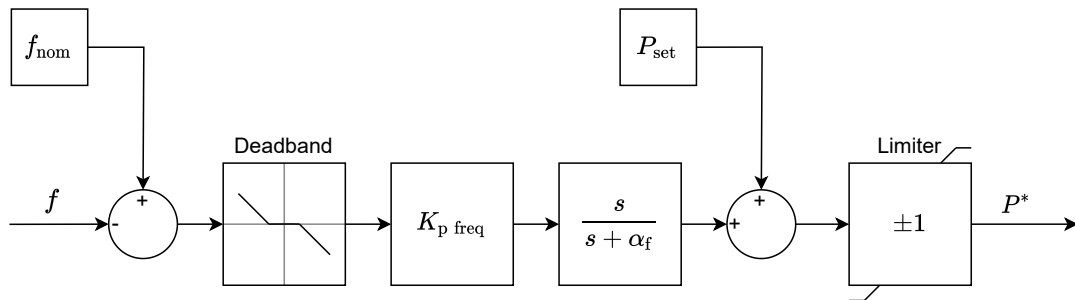


Figure 5.9: Block diagram of adjusted frequency controller with high-pass filter to slowly set the adjusted output active power of the BESS due to a frequency deviation to zero after an event.

6

System Realization

The block diagram for the battery model is introduced along with motivated assumptions regarding battery dynamics. The complete model for controlling the BESS is presented as well as the model for the gas turbines in Rya. Results of verification simulations for the used models are included to motivate the behaviour of various elements of the system.

6.1 Battery Modelling

The battery is modelled as a first-order equivalent circuit model (see Figure 4.2(b)), in order to represent its dynamic response. Data from published estimations of battery ECM parameters to measured data is used [61][62]. The battery is modelled to have changing characteristics with regards to SOC and temperature, as these parameters generally have the most significant impact on battery behaviour. An assumption is made that the battery is contained within a well isolated area with a proper cooling-system. Following is that the temperature during operation can be assumed constant. In reality, the temperature will vary due to several factors, especially the charging or discharging current flowing through the battery. However, this would mainly correspond to a rise in temperature, which would result in a reduced voltage drop across the internal impedance of the battery. Therefore, this would not have a significant impact regarding the charge or discharge speed of the battery, meaning that it is not a detrimental assumption for this analysis. The temperature should for the full system behaviour be monitored carefully, especially to prevent thermal runaway and battery destruction, as the temperature impacts the chemical reactions inside the battery.

The battery model is first realized in Simulink in order to verify the mathematical representation. The battery is discharged with a predefined current in order to study and verify the response of the battery. Once the model is verified to function as intended, it is created in PowerFactory by using the same approach.

A mathematical representation of the battery is constructed as a block diagram shown in Figure 6.1. The block uses the estimated battery current in order to calculate the resulting SOC from charging or discharging. Furthermore, once the SOC is known, the corresponding output voltage of the battery is calculated through the defined relation of battery impedance voltage drop with SOC and temperature.

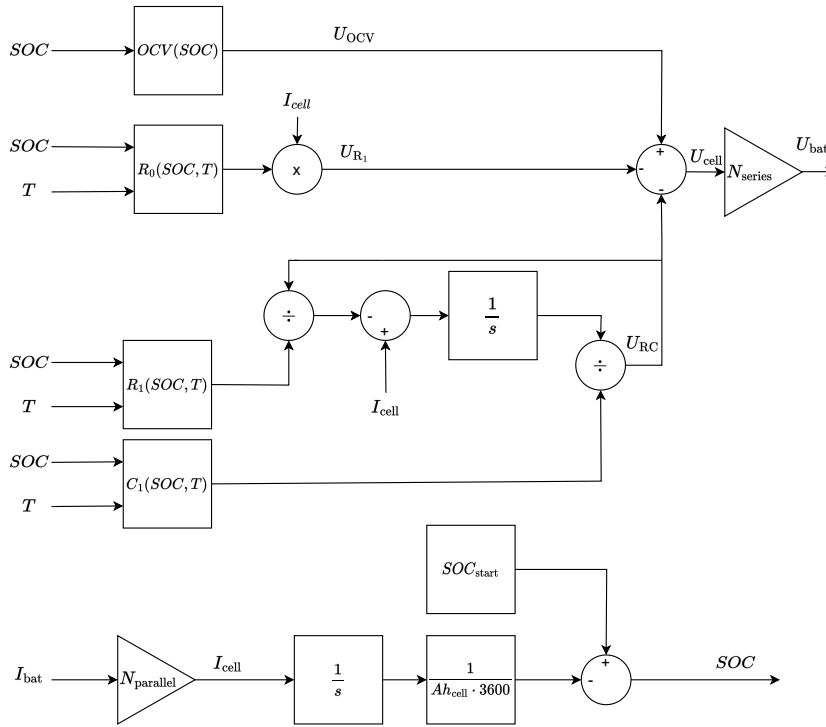


Figure 6.1: Mathematical representation of the battery model. The measured current and temperature are taken as input, where in turn the SOC and resulting battery terminal voltage are found.

6.2 BESS Representation

Due to the complexity of building a converter that has sufficiently low switching harmonics, the BESS representation in the physical grid is simplified. This is done by modelling the grid-forming converter together with the battery as a static generator. The static generator acts corresponding to a set reference voltage which decides the output voltage of the device. The result is that the static generator represents the battery behind an ideal converter. The motivation behind this methodology is that the converter design is not included in this thesis and that the converter design for a real implementation is not yet determined. However, it should be highlighted that the converter has a significant impact for the overall performance of the power quality of the BESS, as well as its limitations during operation.

6.3 Control System Setup

The full control system includes the control of a grid-forming converter as well as the control and model of the battery. This includes active power control, voltage control, frequency control (or an active power setpoint depending on the operational mode), terminal voltage estimation and SOC estimation. A representation of the control system for the study is shown in Figure 6.2. An assumption is made that any required measurement is available for use, mainly being information regarding

the PCC where the BESS connects to the power system and load buses. The flow of active power at the PCC is measured and fed to the active power controller together with a set reference power which is obtained either through a frequency controller or an active power setpoint. The controller then forces the measured active power at the PCC to equal that of the reference and finds the corresponding angular frequency ω and phase angle θ . The phase voltages are measured at the PCC, transformed to $\alpha\beta$ -frame by power-invariant Clarke transformation and then transformed to dq -frame by Park transformation [63]. The magnitude of the dq -voltage is fed into the voltage controller which attempts to keep the voltage close to the nominal system voltage. The output of the voltage controller is then fed to the active power controller in order to set the magnitude of the reference voltage. Using the obtained voltage magnitude and phase angle, the reference voltages are found and fed as inputs to the grid-forming converter. The corresponding output power of the battery is monitored and fed to the battery model in order to find the battery current and monitor the SOC and terminal voltage.

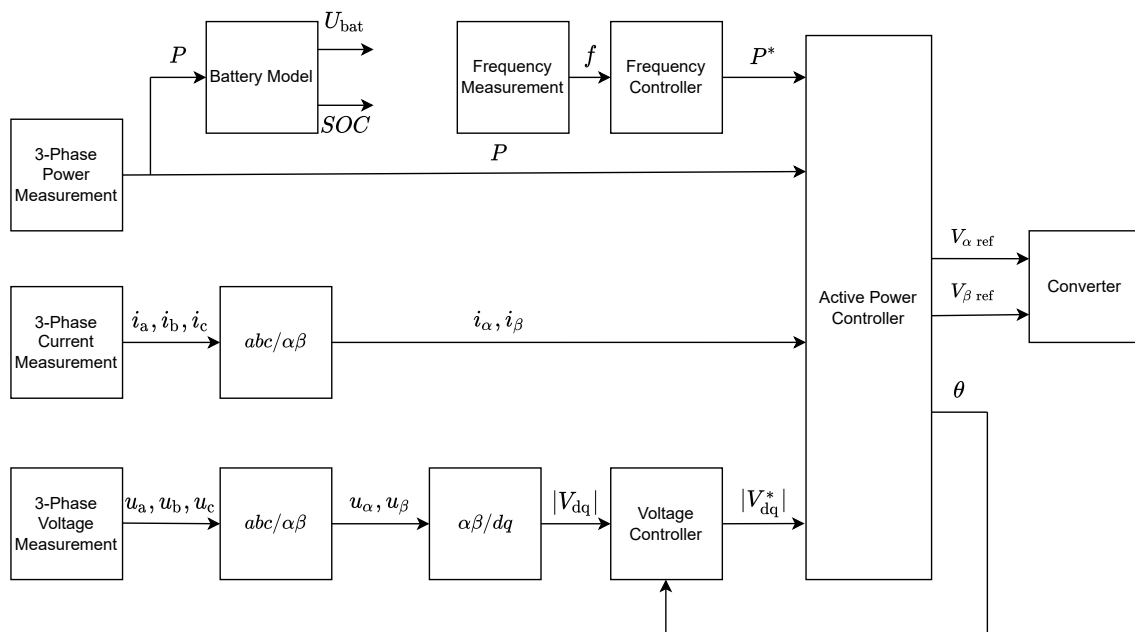


Figure 6.2: Representation of full control system for BESS. This includes measurements of active power, currents and voltages. The measured quantities are transformed to $\alpha\beta$ -frame and dq -frame, and fed to the corresponding control system models.

6.4 Modelling of Gas Turbines in Rya CHP Plant

Due to limitations in available information, the gas turbines of Rya CHP plant are modelled as general gas turbines with commonly used templates. The turbines are in PowerFactory represented by a governor and an excitation system behind a synchronous machine template. The governor estimates the mechanical power of the turbine, and the IEEE GAST-model is used, due to its relative simplicity and

that it is commonly applied [64]. The excitation system estimates the excitation voltage of the machine. In this project, the IEEE AC8B model is used. The result of this approach is that Rya CHP plant is not directly modelled due to its individual characteristics, but seen as a general, arbitrary representation of gas turbines. In order to assure that the characteristics of the gas turbines are realistic, data from a 95 MVA gas turbine in [64] is used for the governor model. The three gas turbines of Rya are aggregated to a single, large gas turbine with a maximum power output of 135 MW. The characteristics of the governor are shown in Table 6.1. In order to confirm that the gas turbine behaves as expected, a load rejection simulation is performed. This is included in Appendix A.

Table 6.1: GAST governor parameter characteristics for reference 95 MVA gas turbine [64].

Parameter	Setting
Permanent droop [p.u.]	0.042
Governor time constant [s]	1.5
Turbine power time constant [s]	0.1
Turbine exhaust temperature time constant [s]	3
Temperature limiter gain [p.u.]	1
Ambient temperature load limit [p.u.]	1
Turbine damping factor [p.u.]	0
Minimum turbine power [p.u.]	-0.02
Maximum turbine power [p.u.]	1
Inertia constant [s]	6.5

6.5 Verification of Model Implementations

This section aims to verify that the derived models function as intended. A constant current discharge and charge test is conducted for the battery. The BESS control system is verified by applying a step in the reference active power.

6.5.1 Battery Model Verification

The battery model is verified through simulations in Simulink where the battery is operating on its own without being connected to a grid. The battery is discharged from its maximum allowed SOC of 0.9 to the minimum of 0.1 and charged vice versa with a constant current of 1C, corresponding to a full discharge or charge in one hour. This is done by connecting a constant corresponding to the rated current of the BESS to the measured current used as input to the battery model. This means that a correct estimation of SOC would indicate that a full discharge or charge will take 60 minutes. The SOC, current, OCV and terminal voltage is calculated and monitored. The profiles of the test are shown in Figure 6.3. The result is verified by analysing the SOC, and it can be seen that the time in order for the battery to discharge respectively charge is 48 minutes. This is expected as the battery SOC range is 80%, while the current is chosen to have a full discharge in 60 minutes.

The result shows the voltage profile at the terminal voltage compared to the OCV, depending on both the SOC at a given moment and the connection between battery impedance to SOC and current.

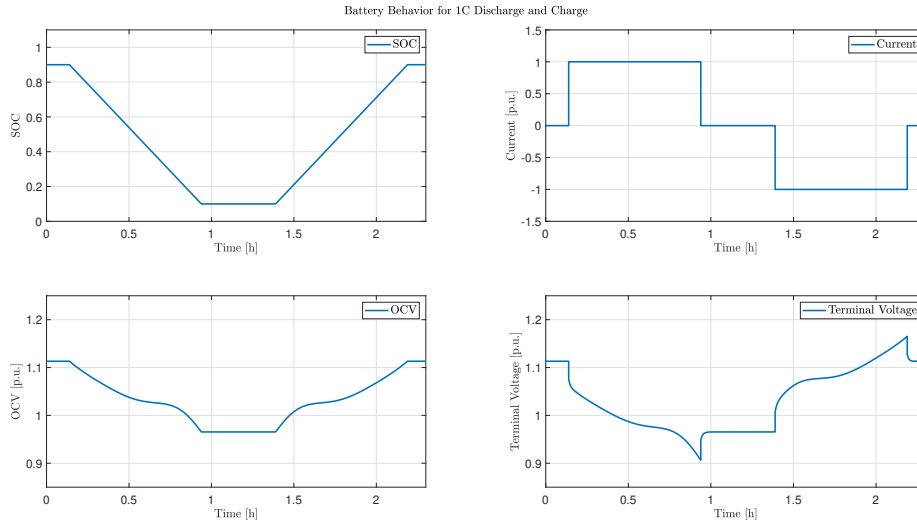


Figure 6.3: Battery SOC-profile, current, OCV and terminal voltage for 1C discharge and charge in a SOC range of 0.9–0.1.

6.5.2 BESS Control System Verification

The control system for the grid-forming converter is verified by applying steps to the reference power which should be followed by that the BESS changes its corresponding output power. Therefore, the frequency controller is replaced by a simple step in active power reference. The system is designed to act as a first-order response to a step change in active power reference. The system used to verify the behaviour for the BESS in PowerFactory is shown in Figure 6.4. A static generator is used to represent the battery behind an ideal converter to remove the impact of switching harmonics. The connecting grid is modelled as an ideal voltage source with an internal series impedance constituted by a resistor and an inductor. The verification is based on that the initial condition for the BESS is to not provide any active power and the resulting active power exchange between the grid and BESS should be zero. At the time of one second in the simulation, the reference power is stepped to one per unit, and stepped back to zero again at four seconds. The resulting active power exchange and reference power with different grid strengths is shown in Figure 6.5. The tuning of the controller is done under the assumption of an infinitely strong grid. This is never true, and Figure 6.5 shows how the accuracy of the tuning changes with the Short-Circuit-Ratio (SCR). A weak grid has a low SCR, and a high equivalent impedance, resulting in a more severe overshoot in active power compared to a strong grid. This shows that the derived controller performs worse in a weak grid while it performs well in strong grid conditions.

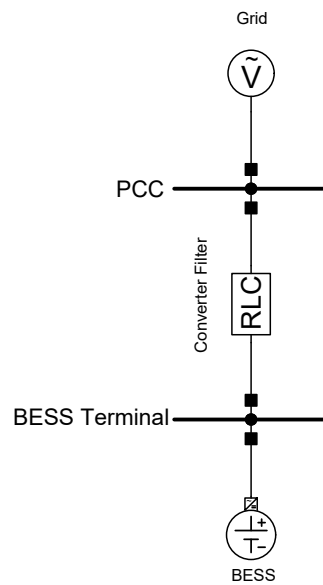


Figure 6.4: Testing system for BESS control consisting of BESS, converter filter and grid.

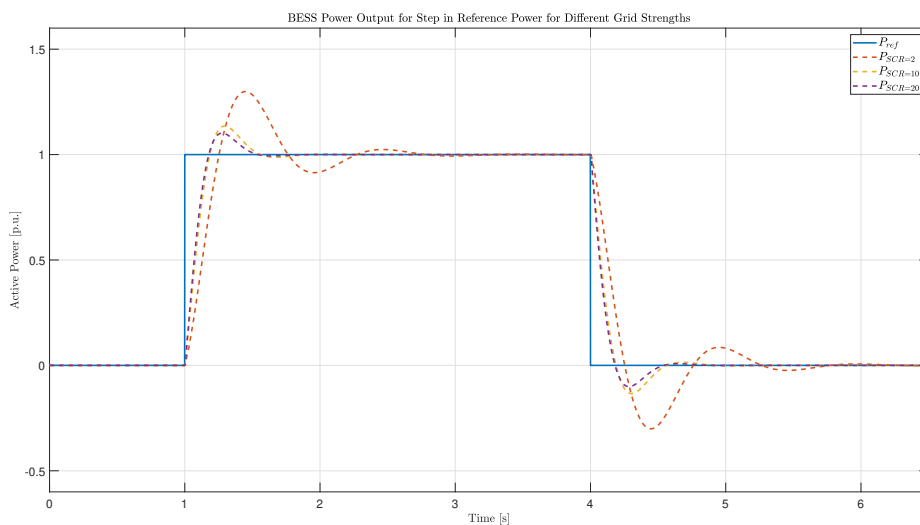


Figure 6.5: Control system response when active power reference is stepped from 0 to 1 p.u. and vice versa for grid strengths with $SCR = 2$, $SCR = 10$ and $SCR = 20$.

6.5.2.1 Effect of Active Damping from Measured Power

The derived control structure from Section 5.2.4 contains an active damping term $P \cdot R_{a1}$ that is added to the output of the PI-controller. As already covered, the purpose of this is to prevent overshoots in active power output when the reference power changes. In Figure 6.5, it can be observed that a weak grid is subject to overshoots even if the damping term is included. Figure 6.6 shows the corresponding

controller response for a strong grid with an SCR of 20 for the derived controller in Section 5.2.4, as well as the controller response if the introduced damping term is removed. The result shows that the damping term efficiently reduces the overshoots and that the controller is subject to severe overshoots even for a strong grid should the damping term be removed. By comparing Figure 6.5 and Figure 6.6, it can be observed that the corresponding controller without active damping for a strong grid performs worse than the controller with active damping in a weak grid.

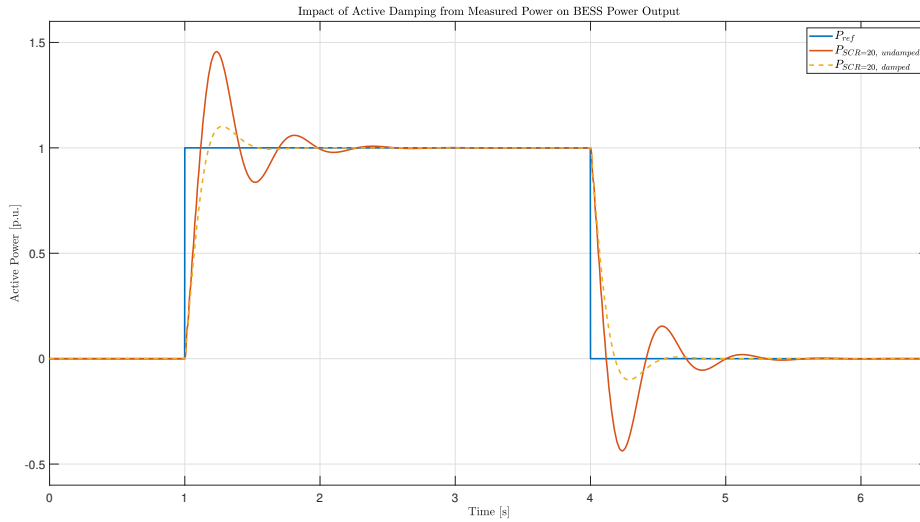


Figure 6.6: Response of BESS when an active power step of 1 p.u. is applied and removed with and without the damping term R_{a1} from the measured power.

6.5.2.2 Effect of Active Damping from Measured Current

In order to reduce oscillations in active power output of the BESS, a damping term is subtracted from the voltage setpoint by using the measured current. The result of removing this damping term is shown in Figure 6.7. It can be observed that the system is subject to high frequency oscillations around the active power setpoint before reaching a steady value if the damping term R_a is removed. This highlights the importance of the damping, as it prevents oscillations which would otherwise be present when the active power setpoint of the BESS changes.

6. System Realization

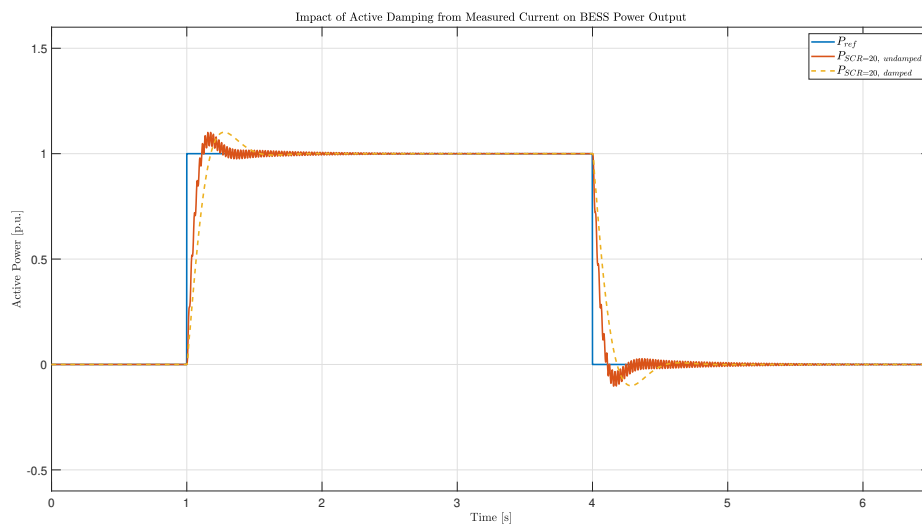


Figure 6.7: Response of BESS when an active power step of 1 p.u. is applied and removed with and without the damping term R_a from the measured current.

7

Simulation Models and Case Studies

This chapter aims to introduce methodology behind the conducted case studies. This includes the categories of grid-connected and islanded operation. The corresponding grid model used in PowerFactory for each simulation case is introduced. An overview of the simulation cases is also presented.

7.1 Overview of Simulation Cases

The studied simulation cases are divided in two subcategories, being grid-connected and islanded operation. Table 7.1 shows the corresponding simulations that have been studied, as well as the section where the procedure of each corresponding case is described. The simulation results are presented in Chapter 8.

Table 7.1: investigated simulation cases, including the corresponding simulation names as well as a reference to the section where each simulation is described in detail. Furthermore, the power system model used for each simulation is presented.

Simulation Case Name	Case Description	Grid Model
Grid-Connected Charging of Ferry	Section 7.2.2	Section 7.2.1
Islanded Charging of Ferry	Section 7.3.2	Section 7.3.1
Frequency Response Improvement	Section 7.3.3	Section 7.3.1
Impacts of Reaching SOC Limits	Section 7.3.4	Section 7.3.1
Frequency Controller Gain	Section 7.3.5	Section 7.3.1
Impact of BESS Inertia Constant	Section 7.3.6	Section 7.3.1

7.2 Grid-Connected Model and Case Studies

As the majority of this project investigates islanded operation, only a simplified simulation is conducted for grid-connected operation. This section introduces the simulation model for this purpose used in PowerFactory as well as the method of the simulation in question.

7.2.1 Simulation Models for Grid-Connected Operation

To investigate the impact on system frequency of connecting the electric ferry to the main grid, the system in Figure 7.1 is used. The model consists of the BESS, electric ferry as well as an external, aggregated grid represented by a hydropower plant. The purpose is to provide a simple model to represent the Swedish power grid in order to analyse if the electric ferry has any impact on the main grid stability. The hydropower unit is assumed to correspond to a sufficient representation of the Swedish power system considering the high penetration of hydropower. For the simulation purpose, the BESS is taken out of service so that only the aggregated generator feeds the electric ferry.

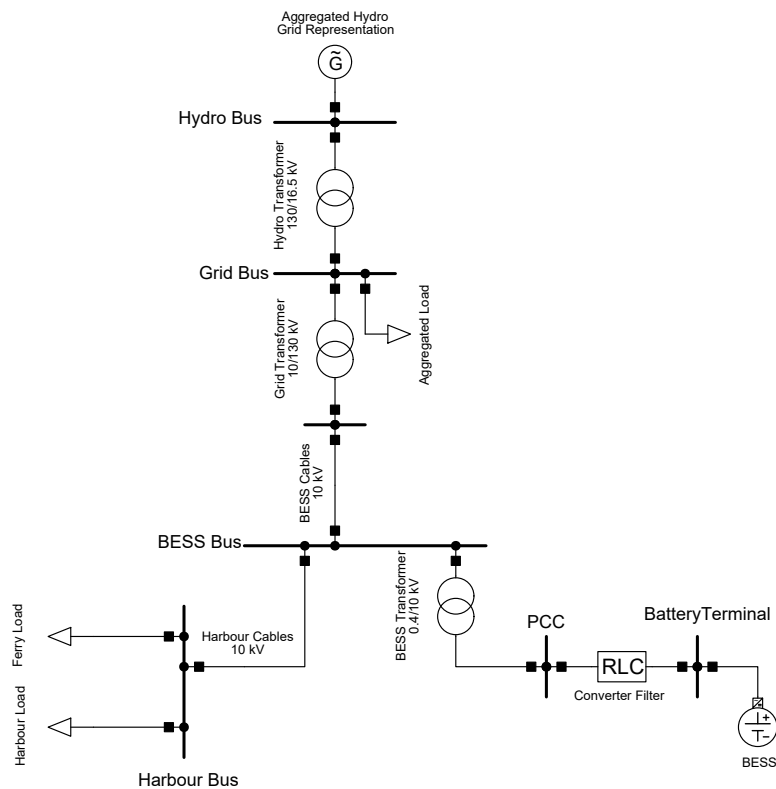


Figure 7.1: One-line diagram for grid-connected operation for frequency response analysis. The grid consists of an aggregated hydropower plant, BESS, electric ferry and aggregated loads.

To investigate how the strength of the synchronous grid affects the eventual need for the BESS, the simulation model in Figure 7.2 is used. For this purpose, the hydropower plant from Figure 7.1 is replaced with an external grid model where the equivalent short-circuit power can be specified and changed accordingly. The estimated, rated short-circuit power at the connection point of the harbour is provided by the local DSO Göteborg Energi [65].

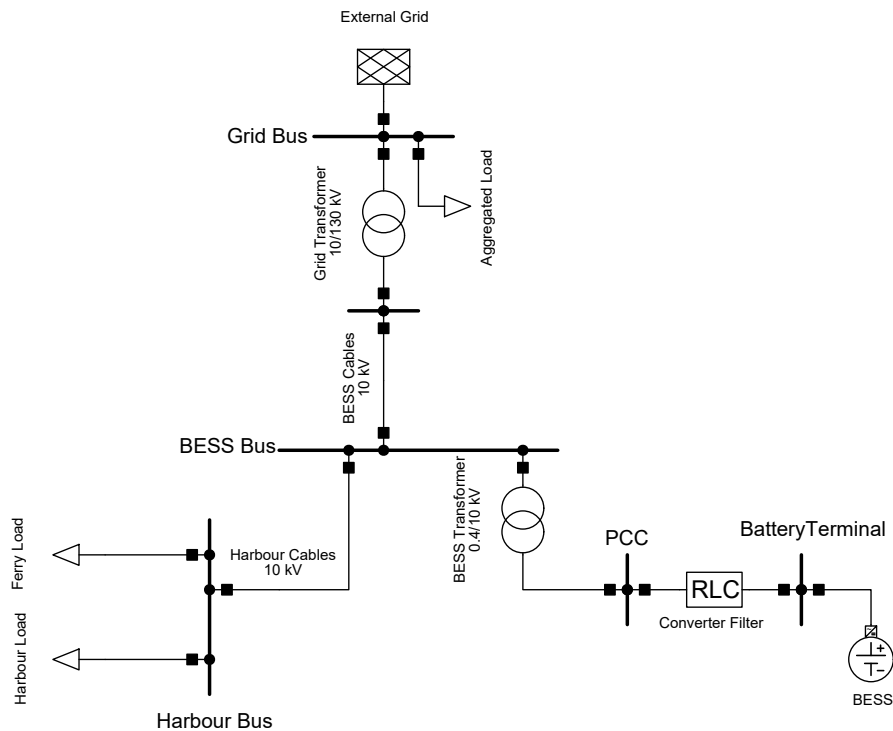


Figure 7.2: One-line diagram for grid-connected operation for Voltage magnitude analysis. The grid consists of an external grid, BESS, electric ferry and aggregated loads.

7.2.2 Grid-Connected Charging of Ferry

In order to understand whether there is a purpose for the BESS to be used for grid stabilization when the ferry is connected or not, the Swedish grid is modelled as an aggregated hydropower plant. The ferry is then connected for the case when the BESS is not present, and the frequency response is analysed. This is because the ferry represents a rather insignificant load compared to the entirety of the power system. Therefore, there may not be a purpose for the BESS to provide stabilizing services for when the ferry is connected. However, the BESS can be used to assist the charging of the ferry if the main grid is heavily loaded such that the harbour is restricted in terms of power exchange from the main grid. For this situation, the BESS can be used to provide the missing active power. This would be a rare occurrence, as the local grid owner is usually able to reliably provide the agreed upon power. The system setup for this simulation is shown in Figure 7.1. Note that the BESS is disconnected from the main grid when the original frequency response is tested.

The simulation is conducted for two cases, being when the synchronous power system is considered according to what is specified from [65] and when the grid is weak where the equivalent short-circuit power is ten times lower. This changes the equivalent impedance that connects the external grid to the harbour and hence the voltage

profile when a current flows from the grid to the harbour when a load is connected.

7.3 Simulation Model and Case Studies for Is- landed Operation

Islanded operation constitutes the majority of the investigated simulation cases. This section introduces the simulation model used for islanded operation in Power-Factory as well as the method behind each simulation.

7.3.1 Simulation Model for Islanded Operation

The setup used for islanded operation is shown in Figure 7.3 and consists of two generating units, being the BESS and the gas turbines from Rya. The grid is designed so that the BESS is connected to a dedicated 10 kV bus. The bus is connected through 10 kV cables to the connection point of the ferry and harbour loads, as well as to the closest substation. The harbour grid and Rya are connected via 10/130 kV transformers. Furthermore, an aggregated load is added on the island 130 kV grid bus to simulate other loads in the islanded grid and motivate that the islanded grid is operating in steady-state prior to the connection of the electric ferry. Cable and transformer data is chosen with regards to standards of Göteborg Energi. Due to confidentiality reasons, the amount of parallel units or cable lengths could not be shared. Therefore, the amount of parallel cables and transformers are chosen such that the maximum estimated power transfer is below the total nominal of the elements. However, the impact of these assumptions on the islanded grid behaviour is very small, mainly due to that the short cable length limits the cables impact. If the physical transmission distance would be longer, the impact would be more significant.

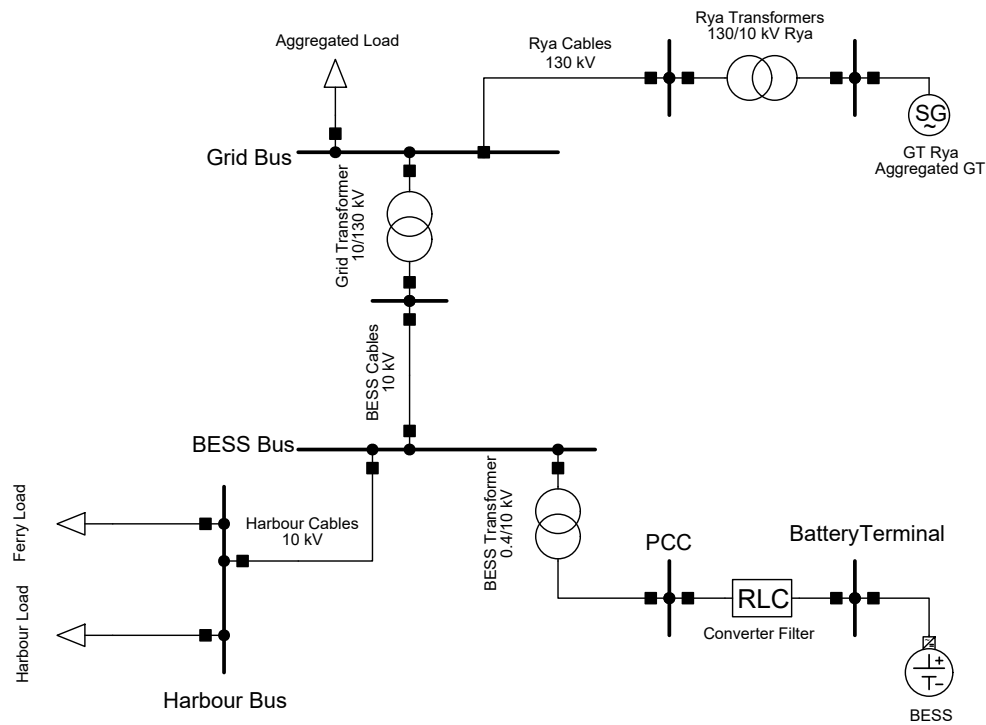


Figure 7.3: One-line diagram for islanded grid used for simulations in PowerFactory, consisting of BESS together with the BESS converter filter as well as gas turbines, electric ferry and aggregated loads.

7.3.2 Islanded Charging of Ferry

The impact of the charging of the ferry becomes significantly more noticeable if the charging occurs for an islanded power system as the ferry represents a larger load in relation to the grid size. Therefore, the islanded grid in Figure 7.3 is used. In order to analyse the impact of the BESS, cases are observed where the grid is only controlled by the gas turbines and when the BESS offers support to stabilize the grid. In order to simulate the grid without BESS, the branch where the BESS is connected is simply taken out of service to create the alternative islanded grid. The ferry is connected by ramping its corresponding active power load during different time windows in order to analyse the frequency response, active power contribution from BESS and gas turbines as well as voltage magnitude at the connection point of the ferry. This simulation is done for two cases, where the ferry is connected by ramping from zero to nominal load within one second and ten seconds respectively. Notable is that a continuous ramping of loads is not available for Electromagnetic Transient (EMT) simulations in PowerFactory, as loads are modelled as fixed, constant impedances. Therefore, ramping is achieved by dividing the ferry in multiple segments of small instantaneous steps to imitate a constant ramping behaviour. This causes the waveforms to appear more abrupt than what in reality would happen, especially for the voltage profile and the slow connection strategy. The corresponding information regarding the two simulations is shown in Figure 7.2.

Table 7.2: Considered connection methods for electric ferry. Two cases are investigated where the ferry is connected fast during a ramp of one second and slow during a ramp of ten seconds respectively.

Case Name	Ramp Duration [s]	Ramping Rate [MW/s]
Fast Ramping	1	40
Slow Ramping	10	4

7.3.3 Frequency Response Improvement

As it may be undesired to continuously discharge the BESS when the electric ferry is connected should there be sufficient power available from the gas turbines, the islanded system response is analysed if the adjusted frequency controller presented in Figure 5.9 is used. For this purpose, the electric ferry is connected as a ramped load from 0 to 40 MW in one second to provide a significant grid event. The purpose of this is to illustrate how the BESS can be used to quickly inject active power to make the islanded grid more robust, without continuous discharge.

7.3.4 Impacts of Reaching SOC Limits

The BESS is set to operate in a SOC range of 0.9–0.1. If a limit is reached through charging or discharging, the BESS will terminate its current operation to not over-charge or over-deplete. The islanded grid response to these actions is analysed in order to understand how the gas turbines will act once the BESS is unable to provide support and must initiate charging, or when charging must be terminated. The impact of hitting the lower SOC limit and initiating charging is investigated by having the BESS provide support to the gas turbines when the electric ferry is connected. The SOC limit is hit and once the gas turbines find a new steady frequency, charging is initiated. The charging power is set such that the battery will charge fully in three hours. The BESS is then charged to the maximum SOC limit, when charging is terminated and regulation support once again initiated.

7.3.5 Frequency Controller Gain

The gain of the frequency controller directly corresponds to the droop setting of the BESS and dictates how much active power that the BESS will inject to a given frequency deviation. In order to show the impact of varying this variable, a simulation of connecting the electric ferry is conducted for two different frequency controller gain settings, being the base-case of $K_{p \text{ freq}} = 25$ and a case where $K_{p \text{ freq}} = 100$. This to illustrate how the parameter impacts the BESS behaviour and showcase benefits and consequences of adjusting the gain.

7.3.6 BESS Virtual Inertia Constant

A benefit of the grid-forming control is as previously mentioned that it allows the BESS to provide virtual inertia to the system and therefore impact the initial RoCoF during an event in the islanded grid. Therefore, to analyse if the BESS is able

to provide significant virtual inertia, the impact of the virtual inertia constant is investigated. A simulation where the electric ferry is connected as a load ramp with a connection time of one second from zero to nominal loading is implemented. The virtual inertia constant is varied in order to investigate if the BESS is able to provide relevant inertia to the islanded system and hence impact the initial RoCoF during an event. The tested cases of virtual inertia constants correspond to a value of $H = 5$ s, $H = 10$ s, $H = 20$ s and $H = 30$ s.

8

Simulation Results

This chapter presents the results for each simulation study introduced in Chapter 7. This includes connection of the electric ferry to the synchronous grid, connection of the electric ferry to the islanded power system, impacts of hitting SOC limits, alternative frequency controller, impact of the frequency controller gain and the virtual inertia constant of the BESS.

8.1 Connection of Electric Ferry to Main Grid

This section aims to investigate if the connection of the electric ferry Stena Elektra has a significant impact on the synchronous power system. The analysis is done for two cases where the grid is first modelled according to data given from Göteborg Energi, and then changed to correspond to a weaker grid. The corresponding system frequency response when the external grid is modelled as an aggregated hydropower plant is investigated. Furthermore, the voltage magnitude where the electric ferry is connected is presented for the estimated grid strengths.

8.1.1 Synchronous System Frequency for Electric Ferry Connection

Figure 8.1 illustrates an estimated synchronous system frequency response to the connection of the electric ferry. The result indicates that the frequency is merely affected by the connection and that the electric ferry corresponds to an insignificant load compared to the synchronous system as a whole. The maximum frequency deviation as a consequence of the connection is within the expected frequency window presented in Figure 3.6 in Section 3.2.2. This means that no action to reduce the impact of the electric ferry on the synchronous power system is required.

8. Simulation Results

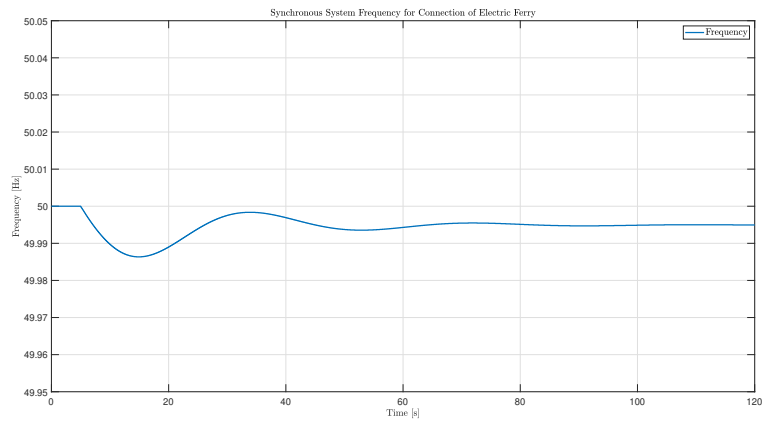


Figure 8.1: Synchronous system frequency when the external grid is modelled as an aggregated hydropower plant and the electric ferry is connected.

8.1.2 Connection of Electric Ferry to Estimated Grid Strength

Figure 8.2 shows the voltage profile at the bus where the electric ferry is connected. At five seconds in the simulation, the ferry is connected as a ramp over one second from zero to nominal loading. The corresponding voltage at the ferry bus decreases equivalently and it can be seen that the resulting voltage is close to the nominal. This is well within the specified limits by the DSO and the connection for this case should not cause problems regarding voltage magnitude. The result shows that the grid strength at the connection point is relatively strong and regardless that the electric ferry represents a relatively large load, the resulting voltage magnitude does not become a problem.

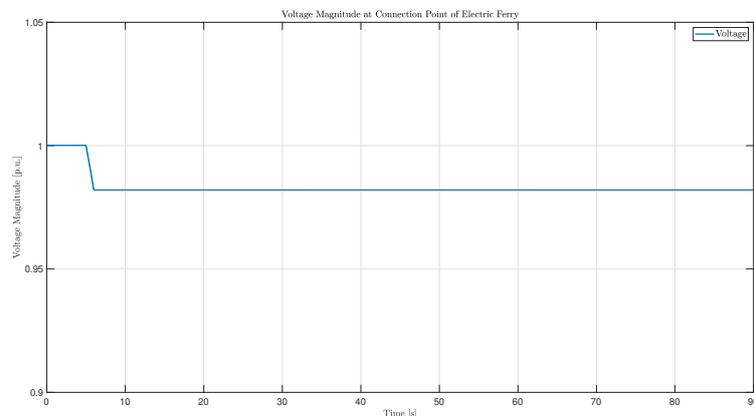


Figure 8.2: Voltage magnitude at electric ferry connection point when external grid strength is chosen according to data from [65].

8.1.3 Connection of Electric Ferry to Weak Grid

A weak grid is prone to more significant voltage magnitude variations when a change in load occurs. Figure 8.3 shows the voltage magnitude at the electric ferry when it is connected to a grid that has an equivalent short-circuit power that is ten times lower than the rated given in [65]. It can be observed that the corresponding voltage drop is now significantly higher than what was found in Figure 8.2 in Section 8.1.2. The maximum allowed voltage drop is 10%, as specified by the DSO in Section 3.2.1. This means that the connection is feasible also for the weak grid configuration and indicates that the electric ferry does not represent a significant enough load to cause severe grid problems.

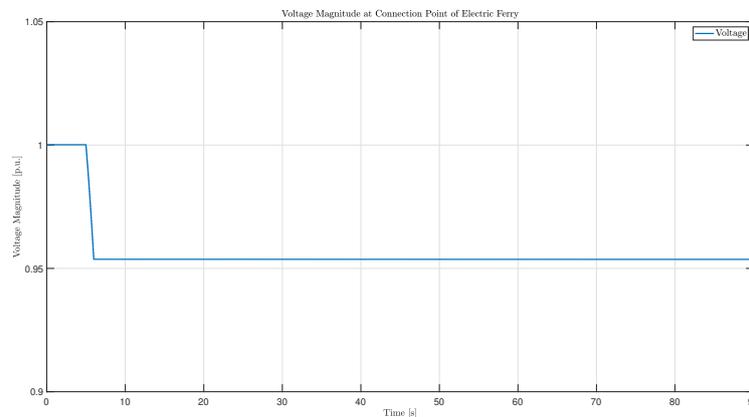


Figure 8.3: Voltage magnitude at harbour connection point when the electric ferry is connected to a weak external grid.

8.2 Connection of Electric Ferry to Islanded Grid

To investigate the impact of the BESS on the islanded power system, the electric ferry is connected for the cases when the BESS is providing support and when it is not present. This in turn is conducted for two cases, where the electric ferry is connected fast and slow respectively.

8.2.1 Fast Connection of Electric Ferry

The result for the simulation case introduced in Section 7.3.2 is presented. Figure 8.4 shows the islanded system behaviour when the BESS is not included in the islanded grid. This includes electric power and mechanical power output of the gas turbines, active power flow to the ferry load, system frequency and voltage magnitude at the point where the electric ferry is connected. At the simulation time of five seconds, the electric ferry is connected as a load and rapidly increases to its rated load. This causes an increased requirement of active power output of the gas turbines. It can be observed that the mechanical power has a slower change than the electric power, which by the swing equation results in a RoCoF until the two are equivalent. The system is prone to a few oscillations before reaching a new steady-state where the

8. Simulation Results

electric and mechanical power are equal at a lower corresponding frequency according to the droop-setting of the gas turbines.

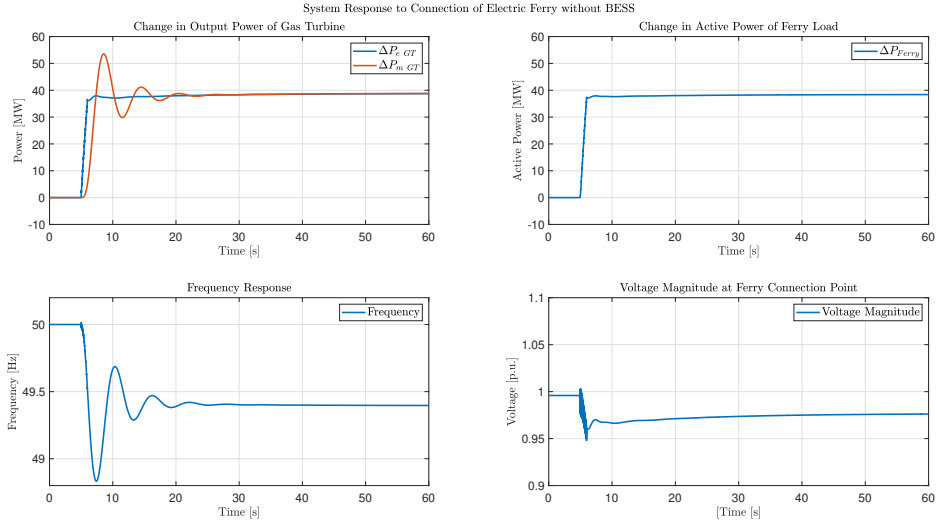


Figure 8.4: Change in electric and mechanical power output of gas turbine, load power of the electric ferry, as well as system frequency response and voltage magnitude at ferry bus for connection of electric ferry when BESS is not present during a fast connection strategy.

The same simulation is carried out for when the BESS is connected to the islanded grid to provide frequency support. The same system properties as previously presented, with the addition of the electric power output of the BESS are shown in Figure 8.5. The result shows that the increased load is now shared between the gas turbines and the BESS, depending on the droop-setting of the two units. The resulting oscillations and overshoots are significantly reduced and the system behaviour is improved.

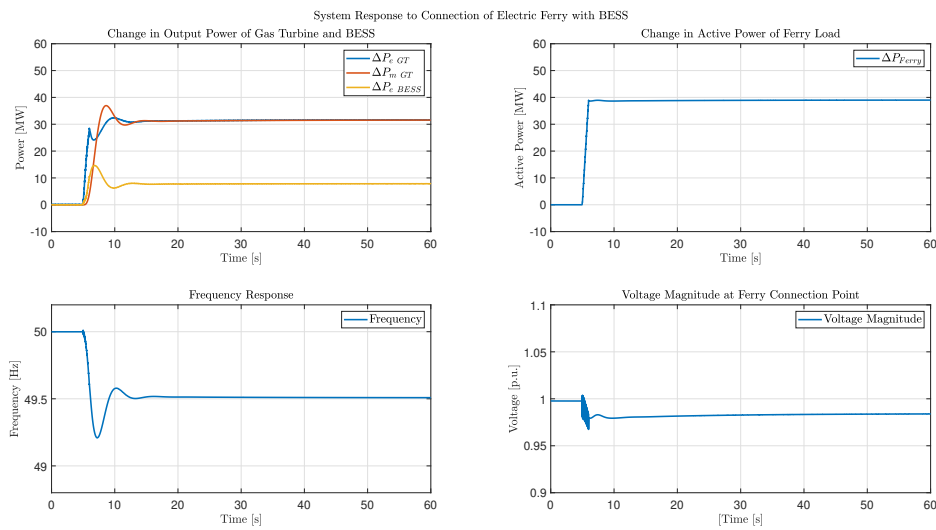


Figure 8.5: Change in electric and mechanical power output of gas turbine, BESS electric power, load power of electric ferry, as well as system frequency response and voltage magnitude at ferry bus for connection of electric ferry when BESS is present during a fast connection strategy.

Figure 8.6 illustrates a comparison of the system response with and without the BESS for the simulation. By comparing the two responses, it becomes clear that the BESS is effective at reducing the magnitude of the initial frequency oscillations. For the case without the BESS, the lowest frequency for this simulation is approximately 48.8 Hz, being outside the allowed frequency window specified in Section 3.1. When the BESS is connected, this response is improved significantly and the system remains within the defined frequency range. Additionally, it can be observed that the final steady-state frequency is closer to 50 Hz when the BESS is connected. This is expected, as the BESS operates so that it continuously discharges should the frequency be outside the deadband of the frequency controller. This results in a lower output power of the gas turbines and hence a frequency that is closer to the nominal. The drawback of this is that the BESS is continuously discharging, resulting in that this operation is not feasible for long time intervals.

8. Simulation Results

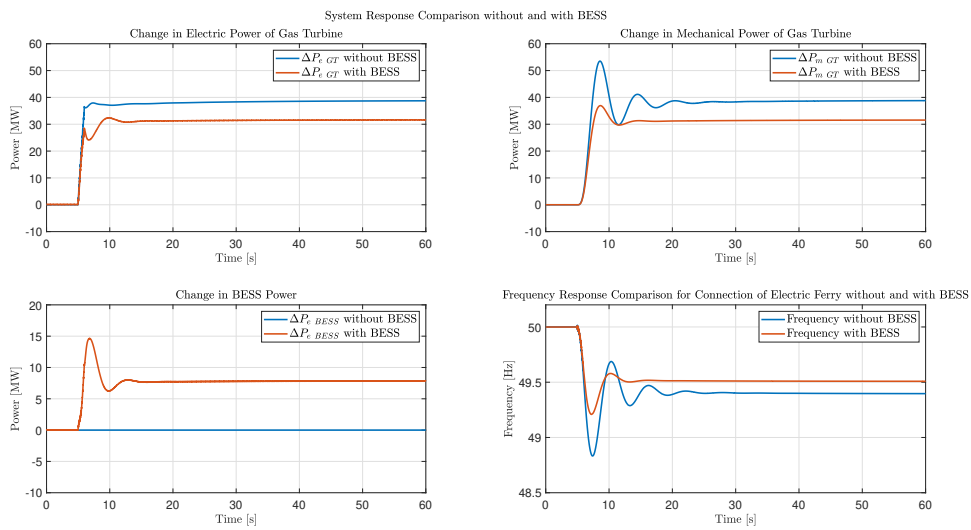


Figure 8.6: System response comparison for islanded power system when BESS is not present and when BESS is used for frequency support during a fast connection strategy.

8.2.2 Slow Connection of Electric Ferry

The connection of the electric ferry can be conducted during a longer time interval. This reduces the initial stress and requirements on the generating units in the grid. Figure 8.7 shows the output electric and mechanical power of the gas turbine, electric ferry load profile, system frequency and voltage magnitude when the ferry is connected at five seconds in the simulation under a ramping behaviour of ten seconds. Comparing the result with the same simulation in Section 8.2.1, it becomes obvious that this ramping behaviour has much less impact on the system and the lowest frequency is not as severe as the previous case. This because the strategy of applying the load is more suitable for the slower dynamics of the gas turbines.

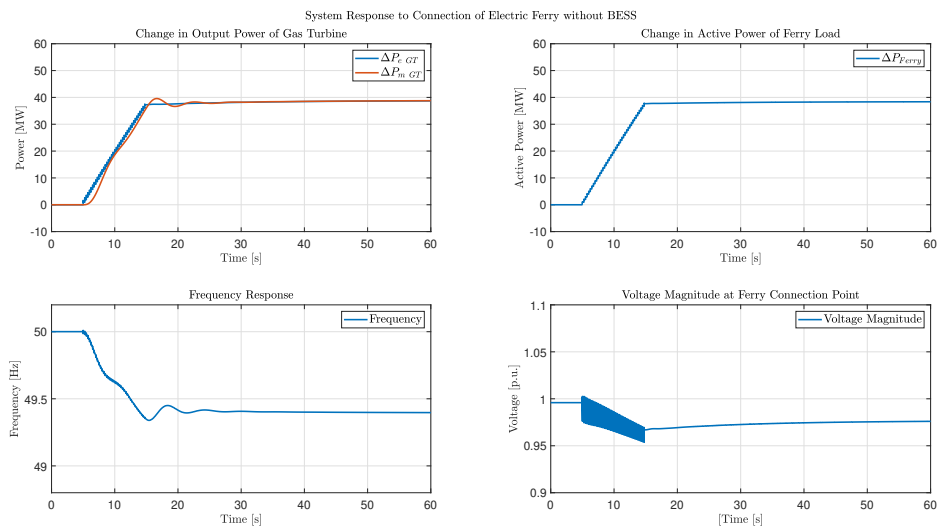


Figure 8.7: Change in electric and mechanical power output of gas turbine, load power of the electric ferry, as well as system frequency response and voltage magnitude at ferry bus for connection of electric ferry when BESS is not present during a slow connection strategy.

Figure 8.8 shows the same system properties with the addition of electric power of the BESS if the BESS is used for frequency support for the same event. As for the case when the ferry is connected during a ramp of one second, the system response is improved as the BESS supports by taking a part of the increased load, resulting in a less severe frequency disturbance.

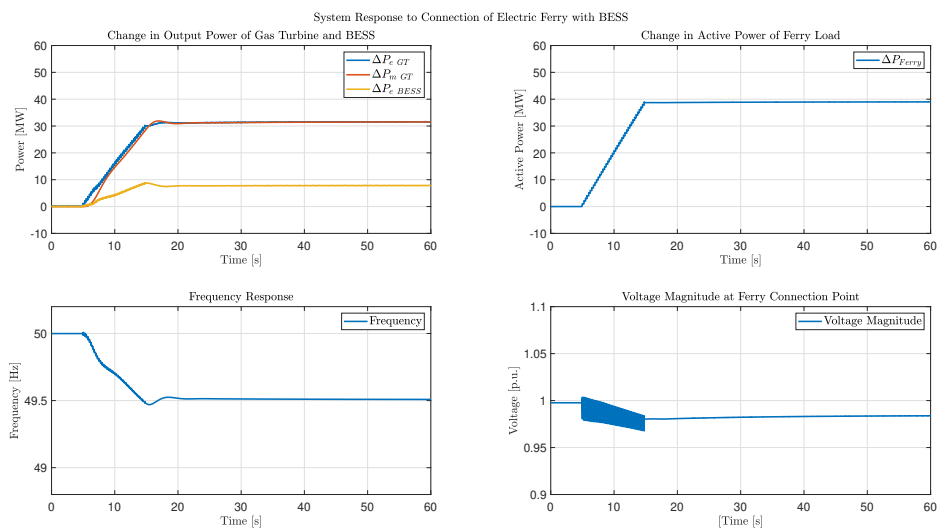


Figure 8.8: Change in electric and mechanical power output of gas turbine, BESS electric power, load power of electric ferry, as well as system frequency response and voltage magnitude at ferry bus for connection of electric ferry when BESS is present during a slow connection strategy.

8. Simulation Results

Figure 8.9 compares the system response for the simulation with and without the BESS. It can be observed that the corresponding frequency response is improved with the BESS. However, much less compared to what has been found in Section 8.2.1. This shows that the BESS provides a more significant benefit for faster events when the dynamics of the gas turbines are too slow.

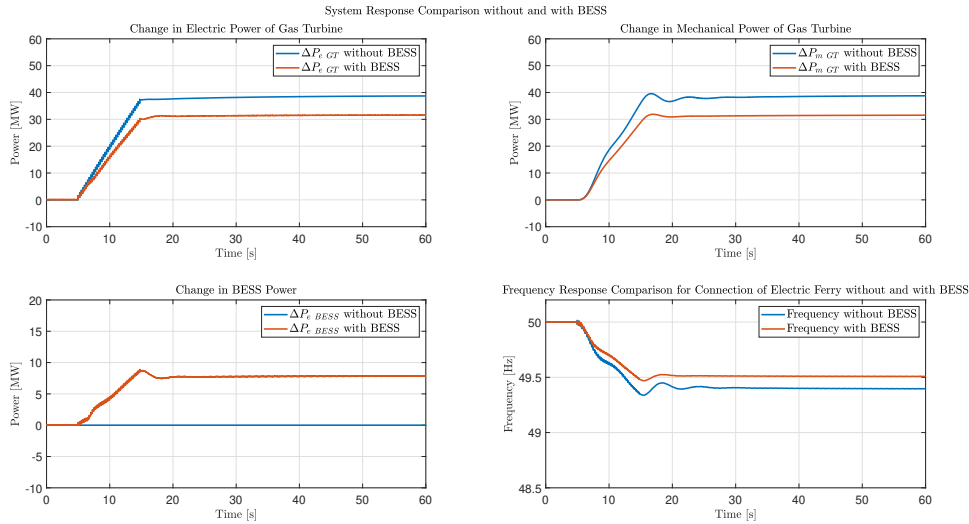


Figure 8.9: System response comparison for islanded power system when BESS is not present and when BESS is used for frequency support during a slow connection strategy.

8.3 State of Charge Limits

The following section presents simulation results for the islanded grid when the BESS reaches its minimum and maximum SOC. The effect on the active power output of the gas turbine and the BESS is observed. Included is the system response to terminating BESS support operation and initiating charging, as well as terminating BESS charging and initiating support.

8.3.1 Lower SOC Limit and Charge Initiation

Figure 8.10 shows the system response when the BESS reaches the minimum allowed SOC and the load must be transferred to the gas turbines. The change in electric as well as mechanical power of the gas turbines is presented. Furthermore, the change in the active power exchange of the BESS with the grid is illustrated, as well as the system frequency and BESS SOC. At 10 seconds in the simulation, the BESS reaches the minimum SOC level of 0.1 by feeding a constant load of 40 MW. This causes the BESS to terminate its possibility of feeding a load, and the result is an increased loading of the gas turbines. As a consequence of this, the system frequency decreases quickly, but the gas turbines are able to find a new steady-state operating point and preserve system stability. At the time of 40 seconds,

charging of the BESS is initiated where the gas turbines are responsible to provide sufficient charging power. This results in an increased frequency deviation, however still within allowed limits. The result shows that the islanded grid is able to remain stable during this operation. However, it should be observed that this simulation is conducted under the assumption that sufficient reserves are available from the gas turbines. If the gas turbines run at maximum load from the beginning of the simulation, it is not possible to transfer the load from the BESS. Nevertheless, this is a fair assumption, as the islanded grid should be structured so that the connected loads at a given can always be sufficiently fed.

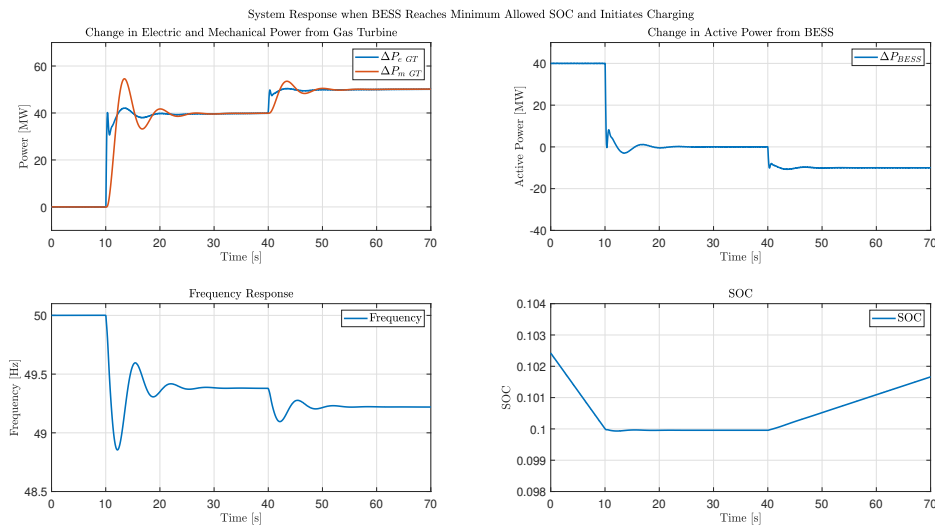


Figure 8.10: Change in electric and mechanical power output of gas turbine, electric power of BESS, system frequency and BESS SOC when minimum SOC is reached and charging is initiated.

8.3.2 Maximum SOC Limit and Support Initialization

When the BESS reaches its maximum allowed SOC of 0.9, charging should be terminated to not overcharge the batteries. A simulation showing the system response when this happens is shown in Figure 8.11. The change in electric and mechanical power from the gas turbines is shown, as well as the active power exchange with the BESS, the system frequency and SOC. At 10 seconds, the BESS reaches the maximum allowed SOC through charging from the gas turbines. This terminates charging and the result is that the load that is supplied by the gas turbines is decreased. Following from this is a frequency increase above the nominal of 50 Hz. The change is relatively minor due to the low charging power of the BESS. The system remains stable and the BESS is once again set to provide frequency support. The resulting system frequency is outside the deadband of the frequency controller and the BESS would for this frequency under normal circumstances provide support by consuming active power. This is however not possible for the presented case, as the BESS is at the maximum SOC and is not allowed to charge any further. Therefore, the BESS cannot for this configuration be used to reduce the resulting

over-frequency from terminating the BESS charging.

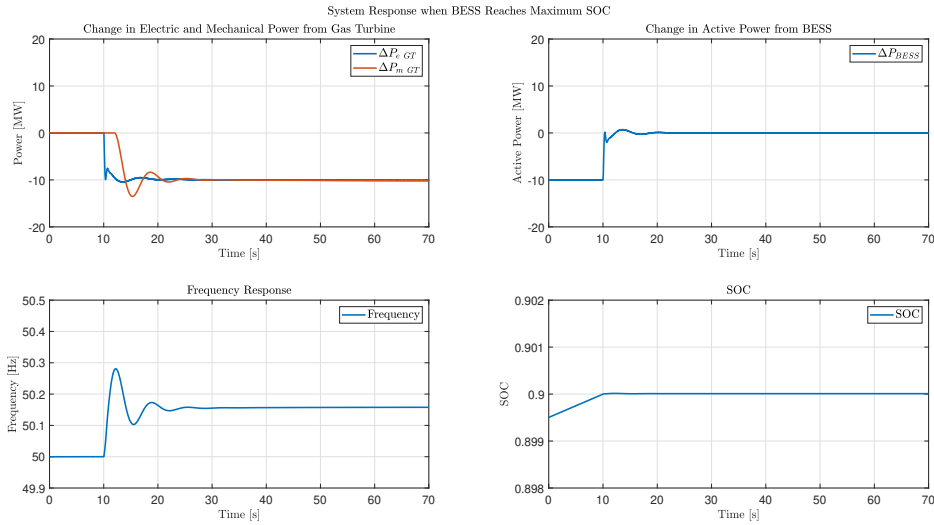


Figure 8.11: Change in gas turbine electric and mechanical power, BESS electric power, system frequency and BESS SOC when Maximum SOC is reached and support is initiated.

8.4 System Response with Alternative Frequency Controller

The result in Section 8.2 shows that the BESS can enhance system behaviour for the assumed configuration. The downside is that it results in a continuous discharge from the BESS. Figure 8.12 illustrates a comparison of the system response for the standard frequency controller presented in Figure 5.8 and the adjusted in Figure 5.9. Displayed is the electric and mechanical power output of the gas turbines, as well as electric power of the BESS and system frequency. The result indicates that both frequency controllers provide a similar response during the initial time instances after an event. The adjusted frequency controller slowly sets the output power of the BESS to zero in order to prevent continuous discharging. This means that the BESS is initially providing support to the system and then slowly transfer the full load increase to the gas turbines, resulting in a lower steady-state frequency. However, still well within allowed limits.

Figure 8.13 presents the comparison in the battery properties of SOC and terminal voltage for the two cases. It can be observed that the standard frequency controller causes a continuous discharge and decline in SOC as well as terminal voltage, while the adjusted controller quickly sets the BESS in an idle position. This gives the possibility of preserving the battery and assuring sufficient SOC while still providing significant support to the islanded grid.

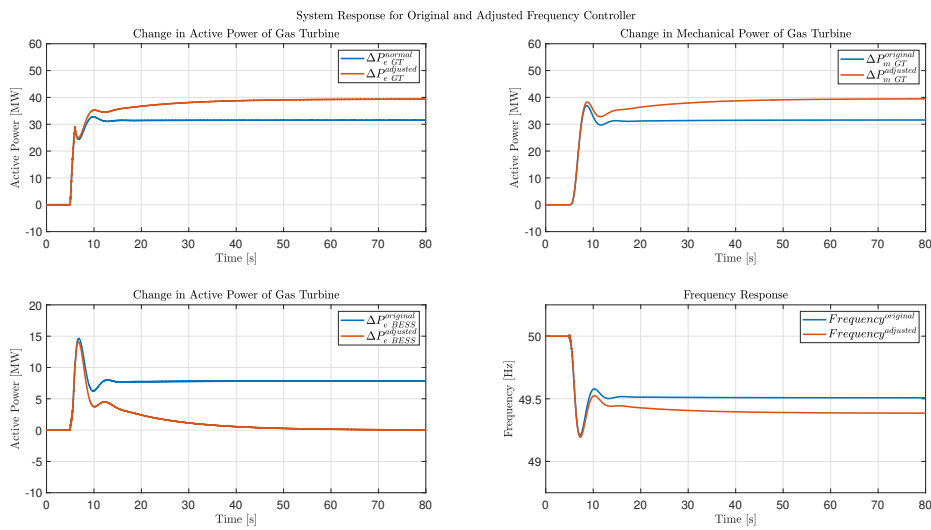


Figure 8.12: Gas turbine electric and mechanical power, BESS electric power and system frequency comparison for the original and adjusted frequency controller.

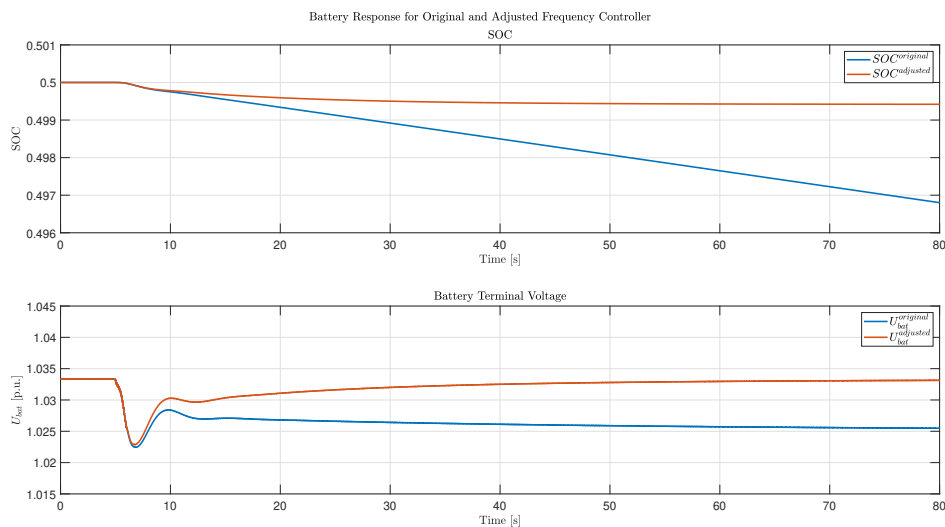


Figure 8.13: Battery SOC and terminal voltage comparison for original and adjusted frequency controller.

8.5 Impact of Frequency Controller Gain

The proportional gain of the frequency controller directly dictates how the BESS output power is set and hence also the profile of energy dissipation during a load event and steady operation. Figure 8.14 illustrates the impact on the system in electric and mechanical output power of the gas turbines, electric power of the BESS and frequency by changing the gain of the frequency controller for the BESS. The base-case has a gain of $K_{p, \text{freq}} = 25$ whereas it is now compared to a value

8. Simulation Results

of $K_{p \text{ freq}} = 100$. It can be observed that the BESS responds with a significantly higher output power when the gain is increased, which further decreases the change in active power of the gas turbines. Following from this, the new steady-state frequency is even closer to 50 Hz, with the consequence of high stress on the BESS in both initial output power and steady-state output power. Figure 8.15 compares the resulting difference in SOC profile and battery terminal voltage, and it can be observed that the increased frequency controller gain increases the rate of change of SOC accordingly.

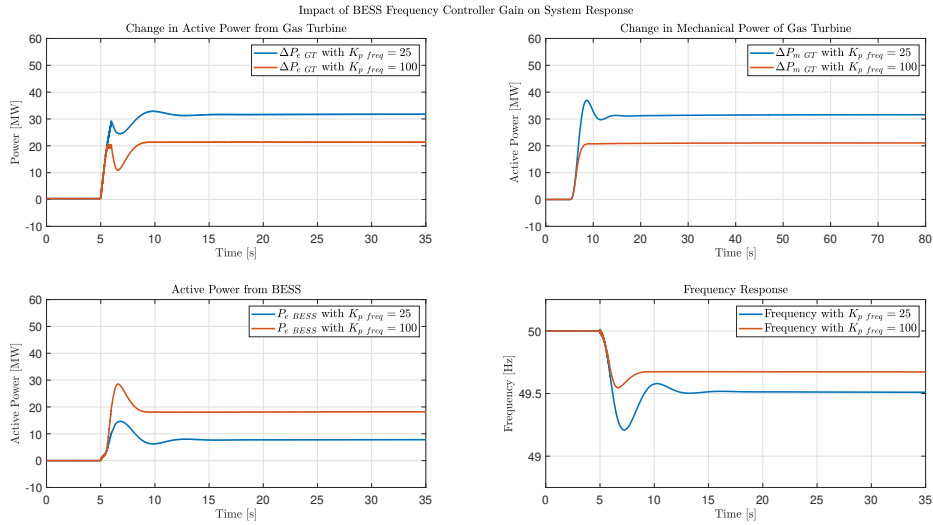


Figure 8.14: Electric and mechanical power output of gas turbines, active power of BESS as well as system frequency when the electric ferry is connected as a ramp over one second from zero to nominal load with BESS frequency controller gain of 25 and 100.

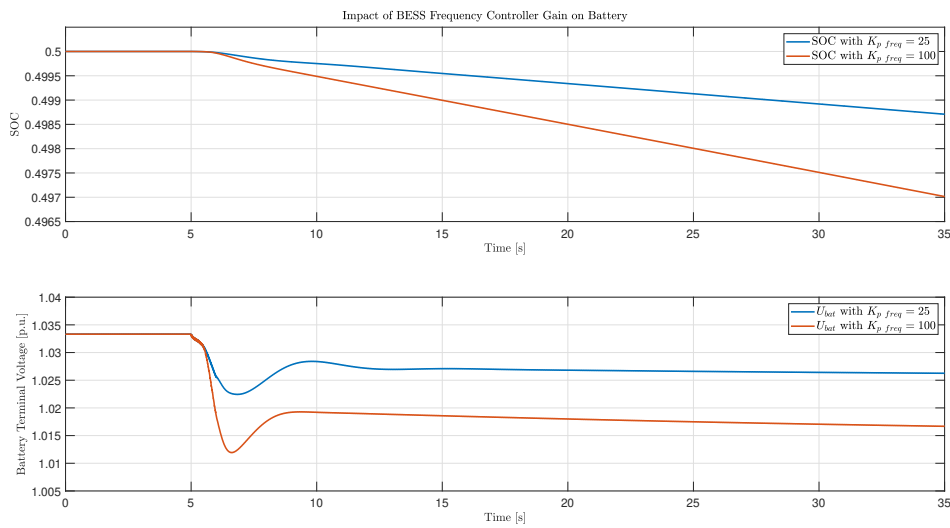


Figure 8.15: SOC and battery terminal voltage when the electric ferry is connected as a ramp over one second from zero to nominal load with BESS frequency controller gain of 25 and 100.

8.6 Impact of BESS Inertia Constant

A benefit of the grid-forming converter control strategy is the possibility of providing virtual inertia to the power system. Figure 8.16 shows the active power output of the BESS as well as the system frequency for four different cases where the virtual inertia is changed. The values of virtual inertia are chosen as $H = 5$ s (base-case), $H = 10$ s, $H = 20$ s and $H = 30$ s. The result shows that a high virtual inertia can have significant impact on the initial RoCoF of the system during an event. The drawback of this is that the initial BESS output power is very high and prone to large overshoots, as the virtual inertia is reflected in the PI-controller gains of the active power controller. This shows that even though the BESS can be manipulated to provide more inertia, it comes with the consequence of significant initial stress on the BESS. An observation that should be done that is not visible in Figure 8.16 is that an increased virtual inertia is expected to bring the consequence of a reduced damping of the system. This would be observable if the simulation is performed in a case where the frequency controller is deactivated and the active power output of the BESS is controlled to be constant so that only the changing virtual inertia constant impacts the system dynamics. For the case shown here, it is not visible due to the regulation of the frequency controller.

8. Simulation Results

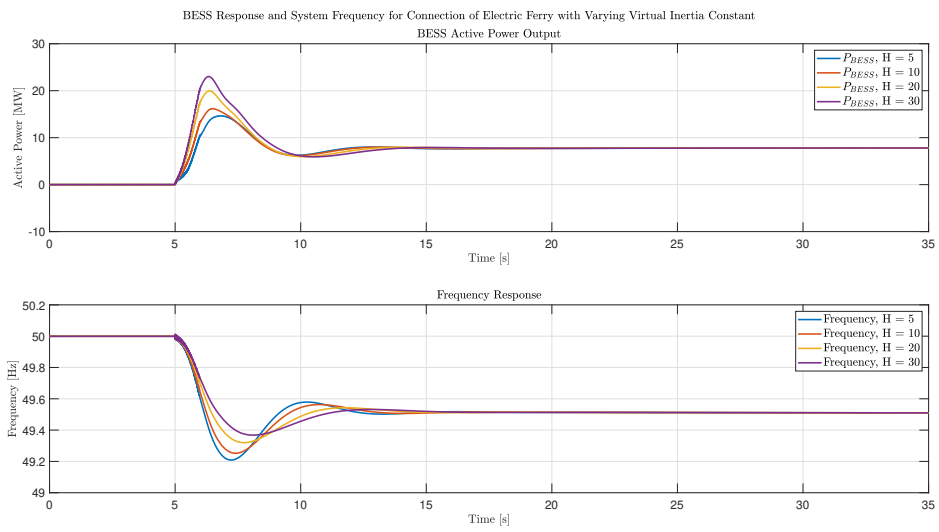


Figure 8.16: Active power output of BESS and system frequency for virtual inertia constant of $H = 5$ s, $H = 10$ s, $H = 20$ s and $H = 30$ s.

9

Discussion

This chapter aims to serve as a discussion around the results that have been obtained. The impact of various BESS tuning is discussed and the benefits as well as drawbacks of BESS are discussed. Additionally, the chapter includes a discussion regarding environmental impact of grid extension versus installing a BESS. Important aspects that have not been included in this work have been summarized as potential future work.

9.1 BESS for Reducing Main Grid Impact

The synchronous Nordic power system is a robust and relatively strong grid with a high amount of power produced from synchronous machines found in hydropower or nuclear plants. The electric ferry has a corresponding charging power of 40 MW, acting as a negligible change for the power system. The equivalent inertia of the Nordic power system considering the generated power is high and the tested cases in this thesis verify that the electric ferry will not cause problems for the stability of the main grid as a whole. Changes continuously occur in the synchronous system, many of which correspond to more significant actions compared to the connection of the electric ferry. This includes connecting large industries or local faults. The resulting change in electrical frequency for the connection of the electric ferry is not noticeable to the synchronous system. Therefore, it is not necessary to connect a BESS in order to improve the system frequency response for the connection of ferry. This is further motivated from that it is required to use a deadband of 100 mHz when providing frequency support for grid disturbed operation. The system electrical frequency is well within this deadband during the connection of the electric ferry, rendering the use of BESS to improve the connection for this purpose moot. With this in mind, the local power system may be affected more significantly by the electric ferry connection. Concluding the outcome of discussions regarding this matter with the DSO Göteborg Energi, it is unlikely that the electric ferry would cause any local grid problems, such as voltage stability issues. This is motivated by that there are already loads more significant than that of the electric ferry that are barely noticeable for the synchronous system stability. Furthermore, the electric ferry is only allowed to consume active and reactive power from the grid according to the grid connection agreement. For this, the DSO assures that during normal circumstances, the local grid is prepared to have sufficient reserves corresponding to the bought connection. Therefore, as long as the connection is approved and considered possible by the DSO and the behaviour of the BESS is in accordance with

the technical requirements, stability issues due to the connection should be unlikely.

Regardless of the BESS being rendered moot to increase the system response for the electric ferry, it can be used for ancillary services such as frequency response. It has been observed that BESS may provide excellent frequency support as a consequence of its fast dynamics. This provides a motivation for installing the BESS regardless of whether it would be required for the electric ferry or not. Nevertheless, this requires further investigation as it becomes a financial matter. If the agreed upon grid connection is sufficient to feed the entirety of the electric ferry, the BESS would only serve to be used for emergency situations or ancillary services. Whether this is beneficial or not depends on the regulation market as well as the manufacturing process and lifetime of the batteries used. If the BESS is continuously cycled by charging the electric ferry, majority of the ageing and corresponding capacity fade owes to cyclic ageing. This significantly reduces the lifetime of the BESS with regards to time, while it also makes effective use of the BESS. If instead the BESS is used for mainly regulating services and emergencies, majority of the lifetime will correspond to calendar ageing. The lifetime in terms of time will be significantly longer. However, the effective lifetime during usage will be expectedly lower as the BESS is often idle. This presents an optimization issue in itself and requires further investigation regarding economical costs of BESS versus charging from the grid, but also the environmental impact of producing the BESS, as well as the charging strategy.

Considering that the Sea Li-ion project aims to use second-life lithium-ion batteries, the environmental impact is expectedly reduced, as the primary manufacturing and material extraction has already been conducted. Consequences may be presented due to ethical reasons, as there may be more important use of the used rare materials. If the current renewable generation trend continues, sufficient green generation may be available from the main grid to make the battery environmental impact significantly less favorable. On the other hand, generation through renewable energy sources such as wind and solar creates an uneven generation, which can be balanced by using storage systems.

9.2 BESS for Islanded Operation

Utilizing a BESS for islanded operation has shown many possible benefits. Section 8.2 shows how the initial frequency response of an islanded system can be significantly improved by using a BESS to provide frequency support. Results show that the magnitude and number of oscillations for a islanded grid event can be significantly reduced by implementing a BESS for frequency control. The BESS possesses fast dynamics and can quickly be regulated in the case of an event on the system such as connecting an additional load. The results also indicate that the BESS can be used to reduce the islanded grid steady-state frequency deviation from that of 50 Hz as it introduces a droop-sharing between the BESS and gas turbines. Nevertheless, operating the grid in a state where the BESS is continuously feeding the system loads is not optimal as it will eventually lead to a complete discharge of the

BESS, thereby limiting the BESS steady-state frequency improvement for long periods of high loading. Following from this operation is also that the islanded grid is not prepared for a future grid event as the BESS can not provide regulative support when it is completely discharged. Furthermore, as the BESS must be charged from the gas turbines, a fully discharged BESS ultimately increases the system loading for the time of the charging. Because of this, it is preferable to use the BESS for support during grid events and slowly phase it out to transfer the full system loading to the gas turbines. This allows reduced frequency transients while the BESS will always be prepared for an upcoming grid event. The BESS can allow the islanded grid to be heavily loaded during scheduled hours where it acts as a generating unit, to be charged when the system load is lower. However, this requires a specific load profile, but it introduces an interesting possibility of allowing high system loading during peak hours of the day. Eventual industries or other facilities connected to the island could run at higher loads during specified, agreed upon time intervals throughout the day.

In Section 8.5, simulations were shown where the islanded grid behaviour was analysed when the gain of the BESS frequency controller was changed. The result indicates that the BESS can adjust the system response to a load increase significantly by introducing a large frequency controller gain. This means that the BESS behaviour can be manipulated in order to assure that the islanded system follows the frequency requirements. By adjusting the frequency gain, the droop-sharing between the gas turbines and BESS is impacted, and it can be used to reduce the initial loading of the gas turbines in the event of a significant load increase. Noteworthy is that it is not recommended to introduce a very large gain, as it will ultimately result in heavy initial loading of the BESS as well as a fast discharge, should the BESS be used in continuous operation. High currents cause significant stress on the BESS and contributes to faster ageing and cell degradation, and in the worst case eventually cell failure. Therefore, it is preferable to set the BESS frequency gain such that the resulting initial frequency response is in agreement with the requirements without resulting in a fast, heavy loading of the BESS. This can still provide benefits of system frequency response behaviour while limiting the BESS loading as has been shown in Section 8.2, where the BESS only supplies approximately 25% of the electric ferry loading.

Section 8.6 investigated if the BESS can contribute to system robustness at the very instance after an event takes place in the islanded grid. The result shows that the BESS can be used to provide significant inertia to the system by adjusting the setting of the PI-controller of the active power controller. This introduces a drawback of high instantaneous power output during the initial RoCoF. This causes a fast initial discharge with a high current flowing through the battery cells. Regardless of this, it shows that the BESS can be manipulated should there be a requirement of reducing system inertia. For the analysed islanded system, the RoCoF is not very high, even for a fast connection of the electric ferry. Concluding from this, the gas turbines have sufficient inertia to preserve system stability when considering the connection of a significant load.

The concluding results from these simulations show that the BESS parameters have a significant impact on its performance and interaction with the grid. This is a major benefit with the BESS, as it can be tuned specifically to a given situation or requirement. Should the BESS be installed for a grid that does not fulfill a grid requirement, it can be tuned in order to make the system agree with what is demanded, given that the system size is small enough for the BESS to have a significant impact. However, it has been observed that the specific tuning of a parameter often comes with a drawback that directly impacts the health of the battery. If the BESS is configured to provide a more significant support during events, it will discharge faster, see higher currents and consume more equivalent life cycles during a shorter time. Therefore, the BESS lifetime is directly impacted by the corresponding tuning. Owing to this, it is preferable to not use the BESS more than required, as it serves no practical purpose to improve grid behaviour significantly above the requirements set from the TSO and DSO.

9.3 Islanded System Demand of BESS

The performed simulations show that the investigated islanded grid is relatively robust even when the BESS is not installed. Gas turbines have a high equivalent inertia constant compared to many other generating units and are seemingly sufficient for the presented grid. The only simulation showing that the gas turbines would not be sufficient on their own is when the electric ferry is connected as a ramp over one second from zero to rated load. However, this simulation is slightly unrealistic, as the connection would generally occur much slower in reality. This would reduce the problems of the slower dynamics of gas turbines and allow them to handle the event better. Additionally, it is not certain that a frequency deviation below 49 Hz for a short time would cause problems for the islanded grid, unless there are very sensitive loads installed.

9.4 BESS or Grid Extension for Environmental Profits

The trend of renewable energy is rapidly becoming a norm and the increasing penetration of generation via solar and wind is a fact. Regardless of this, majority of the generation today is still based on conventional, non-renewable energy sources. This raises an interesting topic regarding the environmental consequences of installing a BESS or alternatively extending the available capacity of the power grid. A grid extension means that the instantaneous available power from the power system must be sufficiently increased in order to match the corresponding increase in load. Unless the required expansion in generation is completely constituted by renewable sources, the installation will cause an increase of non-renewable energy. At the same time, it is difficult to determine whether a full renewable expansion can provide enough steady power to ensure that all grid loads can be supplied at all times. The same

problem can be found if the BESS alternative would be chosen. In order for the BESS to provide an environmental benefit over a grid expansion, the energy for charging the BESS must be provided by renewable sources, otherwise the BESS only presents an additional energy conversion with the only benefit of being able to adjust the system loading by scheduled charging and discharging. Nevertheless, the BESS offers a unique possibility to be used in symbiosis with upcoming renewable generation, where the BESS can potentially be charged during times of high production to be discharged when the generation is low or fluctuating. As it currently stands, a future increased renewable penetration will require some coordinated energy storage system, but whether second-life lithium-ion batteries is the optimal choice for this is not obvious, nor a part of this thesis investigation.

9.5 Future Work

This section aims to introduce suggestions for future work to further extend the study and feasibility of using BESS for islanded power system applications. This includes the implementation of a converter model, black-start capabilities and the possibility to handle faults.

9.5.1 Converter Model

In order to investigate the full behaviour of a BESS for power system applications, the converter connecting the battery and the grid should be modelled so that switching harmonics and non-ideal waveforms can be analysed. In order to be allowed to connect to the grid, there are certain requirements on maximum Total Harmonic Disorder (THD), specified by the DSO. Therefore, it is important to analyse this before installing a BESS to the power system. This task was neglected in this thesis, due to that the required work of designing a suitable converter is too extensive. Furthermore, discussions with Göteborg Energi indicate that harmonics should not pose a problem. Regardless of this, it should be investigated and verified for a real installation.

9.5.2 Black-Start and Seamless Transfer of Islanded Grid

In order to run an islanded grid, the possibility of black-starting and transferring between grid-connected and islanded operation is a necessity. For this thesis, no considerations regarding black-start capabilities have been done, as a realistic black-start strategy requires significant time to develop. The gas turbines are already configured for black-starting and can be used efficiently for this purpose. Using the BESS for the same purpose has not been investigated. However, an interesting topic would be to compare the black-start capability of the gas turbines and BESS respectively in order to investigate which method that represent the best strategy.

9.5.3 BESS Behaviour During Faults

A requirement to connect a unit to the grid is that it is able to operate during a fault without causing problems for the grid or harm to itself. The used BESS model requires modifications in order to function properly for faults. This includes the addition of a virtual impedance and a current controller. This was considered but not implemented as it is outside the scope of the thesis. Noteworthy is that fault-ride through has been conducted in other studies where the BESS for the corresponding situation was found to act properly.

10

Conclusion

This thesis has investigated the possibility of using battery energy storage systems (BESS) for an islanded grid configuration to improve system response. The grid in question is a representation of a future, suggested islanded system including the Port of Gothenburg, Rya combined heat and power plant as well as a BESS. The study was limited to using lithium-ion batteries and no other alternatives were considered.

An electric equivalent circuit model has been successfully modelled to represent the dynamic behaviour of a lithium-ion battery. Additionally, a control structure for a grid-connected BESS has been implemented and verified. It has been found that a BESS possess fast dynamics and can be configured to have significant impact on behaviour of an islanded grid. The impact that various control parameters of the BESS on the system behaviour has been assessed as well as the possible consequences and drawbacks of tuning the BESS for a specific purpose. Additionally, the characteristics of gas turbines have been investigated and the feasibility of using gas turbines to power an islanded grid.

The possibility of providing virtual inertia by BESS has been investigated. Results show that BESS can provide significant inertia to smaller scale islanded grid to reduce the rate-of-change-of-frequency during an event. This has been observed to include the drawback of a high instantaneous power output of the BESS during the initial instances following an event. This causes a high current that leads to a faster discharge and has more impact on battery ageing.

Bibliography

- [1] V. Allgurén, *Personal communication*, May 2022.
- [2] H. Ritchie, *Cars, planes, trains: Where do CO₂ emissions from transport come from?* Our World in Data, 2020. [Online]. Available: <https://ourworldindata.org/co2-emissions-from-transport>.
- [3] *Paris agreement*, United Nations, 2015. [Online]. Available: https://unfccc.int/sites/default/files/english_paris_agreement.pdf.
- [4] *The global electric vehicle market overview in 2022: Statistics and forecasts*, Virta, 2021. [Online]. Available: <https://www.virta.global/global-electric-vehicle-market>.
- [5] *Stena line challenges the shipping industry – by going electric*, May 2021. [Online]. Available: <https://www.stenaline.com/media/stories/stena-line-challenges-the-shipping-industry-by-going-electric/>.
- [6] H. Saadat, *Power system analysis*. PSA Publishing, 2010, ISBN: 9780984543861. [Online]. Available: <https://search.ebscohost.com/login.aspx?direct=true&db=cat07470a&AN=clc.3b1235ca.cd7e.48b8.901e.b6842113772a&site=eds-live&scope=site&authtype=guest&custid=s3911979&groupid=main&profile=eds>.
- [7] *Sea li-ion*, European Commission, 2019. [Online]. Available: <https://ec.europa.eu/inea/en/connecting-europe-facility/cef-transport/2019-eu-tm-0097-s>.
- [8] M. Ramírez, R. Castellanos, J. G. Calderón, and O. P. Malik, “Battery energy storage for frequency support in the bcs electric power system,” in *2018 IEEE PES Transmission Distribution Conference and Exhibition - Latin America (T D-LA)*, 2018, pp. 1–5. DOI: 10.1109/TDC-LA.2018.8511691.
- [9] H.-J. Moon, A.-Y. Yun, E.-S. Kim, and S.-I. Moon, “An analysis of energy storage systems for primary frequency control of power systems in south korea,” *Energy Procedia*, vol. 107, pp. 116–121, 2017, 3rd International Conference on Energy and Environment Research, ICEER 2016, 7-11 September 2016, Barcelona, Spain, ISSN: 1876-6102. DOI: <https://doi.org/10.1016/j.egypro.2016.12.143>. [Online]. Available: <https://www.sciencedirect.com/science/article/pii/S1876610216317325>.
- [10] V. K. Garg and S. Sharma, “Overview on microgrid system,” in *2018 Fifth International Conference on Parallel, Distributed and Grid Computing (PDGC)*, 2018, pp. 694–699. DOI: 10.1109/PDGC.2018.8745849.
- [11] *Stena elektra — from vision to vessel*, Jun. 2021. [Online]. Available: <https://www.stenaline.com/stena-elektra-from-vision-to-vessel/>.

- [12] S. Anwar, M. Y. I. Zia, M. Rashid, G. Z. d. Rubens, and P. Enevoldsen, "Towards ferry electrification in the maritime sector," *Energies*, vol. 13, no. 24, 2020, ISSN: 1996-1073. DOI: 10.3390/en13246506. [Online]. Available: <https://www.mdpi.com/1996-1073/13/24/6506>.
- [13] H. Tistrand, *Personal communication*, May 2022.
- [14] J. Karlsson, *Personal communication*, Apr. 2022.
- [15] *Det får ni för elnätsavgiften*, Feb. 2022. [Online]. Available: <https://www.goteborgenergi.se/foretag/vara-nat/elnat/elnatsavgiften>.
- [16] Göteborg Energi AB, "Miljörapport 2020 Rya Kraftvärmeverk," Gothenburg, Sweden, Tech. Rep. 10-2021-0064, 2020. [Online]. Available: <https://www.goteborgenergi.se/Files/Webb20/Kategoriserad%5C%20information/Informationsmaterial/Milj%5C%C3%5C%B6rapporter/2020/MR%5C%20Rya%5C%20kraftv%5C%C3%5C%A4rmeverk%5C%202020.pdf?TS=637570015933112579>.
- [17] J. Wickström, "Rya kraftvärmeverk testar nya bränslen i gasturbinerna," *Tidningen Energi*, Jan. 2021. [Online]. Available: <https://www.energi.se/artiklar/rya-kraftvarmeverk-testar-nya-branslen-i-gasturbinerna/>.
- [18] *Miljötillståndsansökan biokraftvärme rya*, 2022. [Online]. Available: <https://www.goteborgenergi.se/om-oss/vad-vi-gor/miljotillstandsansokan-biokraftverk-rya>.
- [19] L. Meegahapola and D. Flynn, "Gas turbine modelling for power system dynamic simulation studies," in Dec. 2014, pp. 175–195, ISBN: 978-3-319-12957-0. DOI: 10.1007/978-3-319-12958-7_8.
- [20] Energimarknadsinspektionen, *Energimarknadsinspektionens författningssamling*, Aug. 2013. [Online]. Available: <https://www.ei.se/om-oss/publikationer/publikationer/foreskrifter-el/2013/foreskrift-eifs-20131>.
- [21] "Requirement for minimum inertia in the nordic power system," European Network of Transmission System Operators for Electricity, Tech. Rep., Jun. 2021. [Online]. Available: <https://www.svk.se/contentassets/e142bebe095c42b18902e7f8c6ef1a87/requirement-for-minimum-inertia-in-the-nordic-power-system---2021.pdf>.
- [22] Energimarknadsinspektionen, *Energimarknadsinspektionens författningssamling*, Dec. 2018. [Online]. Available: <https://ei.se/om-oss/nyheter/2022/2022-01-21-oversyn-av-de-nationella-kraven-om-natanslutning-av-generatorer---valkommen-med-synpunkter>.
- [23] *Kontrollrummet*, Svenska Kraftnät, 2022. [Online]. Available: <https://www.svk.se/om-kraftsystemet/kontrollrummet/>.
- [24] "Network code for requirements for grid connection applicable to all generators," European Network of Transmission System Operators for Electricity, Tech. Rep., Jun. 2012. [Online]. Available: <https://extranet.acer.europa.eu/Media/News/Documents/120626%5C%20-%5C%20NC%5C%20RfG%5C%20-%5C%20Requirements%5C%20in%5C%20the%5C%20context%5C%20of%5C%20present%5C%20practices.pdf>.
- [25] S. Kraftnät, *Frekvenshållningsreserv normaldrift (fcr-n)*, May 2022. [Online]. Available: <https://www.svk.se/aktorsportalen/systemdrift-elmarknad/information-om-stodtjanster/fcr-n/>.

- [26] —, *Frekvenshållningsreserv störning uppreglering (fcr-d upp)*, May 2022. [Online]. Available: <https://www.svk.se/aktorsportalen/systemdrift-elmarknad/information-om-stodtjanster/fcr-d-upp/>.
- [27] —, *Frekvenshållningsreserv störning nedreglering (fcr-d ned)*, May 2022. [Online]. Available: <https://www.svk.se/aktorsportalen/systemdrift-elmarknad/information-om-stodtjanster/fcr-d-ned/>.
- [28] International Energy Agency, *Renewables are on track to set new records in 2021*, 2021. [Online]. Available: <https://www.iea.org/reports/global-energy-review-2021/renewables>.
- [29] M. Benidris and J. Mitra, “Enhancing stability performance of renewable energy generators by utilizing virtual inertia,” in *2012 IEEE Power and Energy Society General Meeting*, 2012, pp. 1–6. DOI: 10.1109/PESGM.2012.6345734.
- [30] J. F. Peters, M. Baumann, B. Zimmermann, J. Braun, and M. Weil, “The environmental impact of li-ion batteries and the role of key parameters – a review,” *Renewable and Sustainable Energy Reviews*, vol. 67, pp. 491–506, 2017, ISSN: 1364-0321. DOI: <https://doi.org/10.1016/j.rser.2016.08.039>. [Online]. Available: <https://www.sciencedirect.com/science/article/pii/S1364032116304713>.
- [31] Göteborg Energi, *Göteborg energi välkomnar batterifabriken till göteborg*, 2022. [Online]. Available: <https://www.goteborgenergi.se/i-var-stad/artike1bank/vi-valkomnar-batterifabriken>.
- [32] M. Shen and Q. Gao, “A review on battery management system from the modeling efforts to its multiapplication and integration,” *International Journal of Energy Research*, vol. 43, no. 10, pp. 5042–5075, 2019. DOI: <https://doi.org/10.1002/er.4433>. eprint: <https://onlinelibrary.wiley.com/doi/pdf/10.1002/er.4433>. [Online]. Available: <https://onlinelibrary.wiley.com/doi/abs/10.1002/er.4433>.
- [33] X. Hua, C. Zhang, and G. Offer, “Finding a better fit for lithium ion batteries: A simple, novel, load dependent, modified equivalent circuit model and parameterization method,” *Journal of Power Sources*, vol. 484, p. 229 117, 2021, ISSN: 0378-7753. DOI: <https://doi.org/10.1016/j.jpowsour.2020.229117>. [Online]. Available: <https://www.sciencedirect.com/science/article/pii/S0378775320314129>.
- [34] X. Hu, S. Li, and H. Peng, “A comparative study of equivalent circuit models for li-ion batteries,” *Journal of Power Sources*, vol. 198, pp. 359–367, 2012, ISSN: 0378-7753. DOI: <https://doi.org/10.1016/j.jpowsour.2011.10.013>. [Online]. Available: <https://www.sciencedirect.com/science/article/pii/S0378775311019628>.
- [35] A. Nyman, T. G. Zavalis, R. Elger, M. Behm, and G. Lindbergh, “Analysis of the polarization in a li-ion battery cell by numerical simulations,” *Journal of The Electrochemical Society*, vol. 157, no. 11, A1236, 2010. DOI: 10.1149/1.3486161. [Online]. Available: <https://doi.org/10.1149/1.3486161>.
- [36] L. Zhang, H. Peng, Z. Ning, Z. Mu, and C. Sun, “Comparative research on rc equivalent circuit models for lithium-ion batteries of electric vehicles,” *Applied Sciences*, vol. 7, no. 10, 2017, ISSN: 2076-3417. DOI: 10.3390/app7101002. [Online]. Available: <https://www.mdpi.com/2076-3417/7/10/1002>.

- [37] Y. Xie, W. Li, Y. Yang, and F. Feng, "A novel resistance-based thermal model for lithium-ion batteries," *International Journal of Energy Research*, vol. 42, no. 14, pp. 4481–4498, 2018. DOI: <https://doi.org/10.1002/er.4193>. eprint: <https://onlinelibrary.wiley.com/doi/pdf/10.1002/er.4193>. [Online]. Available: <https://onlinelibrary.wiley.com/doi/abs/10.1002/er.4193>.
- [38] S. Ma, M. Jiang, P. Tao, C. Song, J. Wu, J. Wang, T. Deng, and W. Shang, "Temperature effect and thermal impact in lithium-ion batteries: A review," *Progress in Natural Science: Materials International*, vol. 28, no. 6, pp. 653–666, 2018, ISSN: 1002-0071. DOI: <https://doi.org/10.1016/j.pnsc.2018.11.002>. [Online]. Available: <https://www.sciencedirect.com/science/article/pii/S1002007118307536>.
- [39] X. Tang, X. Mao, J. Lin, and B. Koch, "Li-ion battery parameter estimation for state of charge," in *Proceedings of the 2011 American Control Conference*, 2011, pp. 941–946. DOI: 10.1109/ACC.2011.5990963.
- [40] E. Wikner, E. Björklund, J. Fridner, D. Brandell, and T. Thiringer, "How the utilised soc window in commercial li-ion pouch cells influence battery ageing," *Journal of Power Sources Advances*, vol. 8, p. 100054, 2021, ISSN: 2666-2485. DOI: <https://doi.org/10.1016/j.powera.2021.100054>. [Online]. Available: <https://www.sciencedirect.com/science/article/pii/S2666248521000093>.
- [41] J. Vetter, P. Novák, M. Wagner, C. Veit, K.-C. Möller, J. Besenhard, M. Winter, M. Wohlfahrt-Mehrens, C. Vogler, and A. Hammouche, "Ageing mechanisms in lithium-ion batteries," *Journal of Power Sources*, vol. 147, no. 1, pp. 269–281, 2005, ISSN: 0378-7753. DOI: <https://doi.org/10.1016/j.jpowsour.2005.01.006>. [Online]. Available: <https://www.sciencedirect.com/science/article/pii/S0378775305000832>.
- [42] M. Petzl, M. Kasper, and M. A. Danzer, "Lithium plating in a commercial lithium-ion battery – a low-temperature aging study," *Journal of Power Sources*, vol. 275, pp. 799–807, 2015, ISSN: 0378-7753. DOI: <https://doi.org/10.1016/j.jpowsour.2014.11.065>. [Online]. Available: <https://www.sciencedirect.com/science/article/pii/S0378775314018928>.
- [43] D.-I. Stroe, V. Knap, M. Swierczynski, A.-I. Stroe, and R. Teodorescu, "Operation of a grid-connected lithium-ion battery energy storage system for primary frequency regulation: A battery lifetime perspective," *IEEE Transactions on Industry Applications*, vol. 53, no. 1, pp. 430–438, 2017. DOI: 10.1109/TIA.2016.2616319.
- [44] B. Li, Y. Jiang, and G. Li, "Maximum cycle-life equalization control strategy for lithium-ion battery," in *2021 24th International Conference on Electrical Machines and Systems (ICEMS)*, 2021, pp. 2282–2287. DOI: 10.23919/ICEMS52562.2021.9634550.
- [45] T. Bandhauer, S. Garimella, and T. Fuller, "A critical review of thermal issues in lithium-ion batteries," *Journal of The Electrochemical Society*, vol. 158, R1, Jan. 2011. DOI: 10.1149/1.3515880.

-
- [46] P. Keil et al, "Calendar aging of lithium-ion batteries," vol. 163, 2016. DOI: <https://doi.org/10.1149/2.0411609jes>. [Online]. Available: <https://iopscience.iop.org/article/10.1149/2.0411609jes/pdf>.
- [47] M. Abdel-Monem, O. Hegazy, N. Omar, K. Trad, P. Van den Bossche, and J. Van Mierlo, "Lithium-ion batteries: Comprehensive technical analysis of second-life batteries for smart grid applications," in *2017 19th European Conference on Power Electronics and Applications (EPE'17 ECCE Europe)*, 2017, P.1–P.16. DOI: 10.23919/EPE17ECCEEurope.2017.8099385.
- [48] E. Martinez-Laserna, E. Sarasketa-Zabala, D.-I. Stroe, M. Swierczynski, A. Warnecke, J. Timmermans, S. Goutam, and P. Rodriguez, "Evaluation of lithium-ion battery second life performance and degradation," in *2016 IEEE Energy Conversion Congress and Exposition (ECCE)*, 2016, pp. 1–7. DOI: 10.1109/ECCE.2016.7855090.
- [49] E. Martinez-Laserna, E. Sarasketa-Zabala, I. Villarreal Sarria, D.-I. Stroe, M. Swierczynski, A. Warnecke, J.-M. Timmermans, S. Goutam, N. Omar, and P. Rodriguez, "Technical viability of battery second life: A study from the ageing perspective," *IEEE Transactions on Industry Applications*, vol. 54, no. 3, pp. 2703–2713, 2018. DOI: 10.1109/TIA.2018.2801262.
- [50] N.-B. Lai, A. Tarrasó, G. N. Baltas, L. V. Marin Arevalo, and P. Rodriguez, "External inertia emulation controller for grid-following power converter," *IEEE Transactions on Industry Applications*, vol. 57, no. 6, pp. 6568–6576, 2021. DOI: 10.1109/TIA.2021.3108350.
- [51] Y. Zuo, Z. Yuan, F. Sossan, A. Zecchino, R. Cherkaoui, and M. Paolone, "Performance assessment of grid-forming and grid-following converter-interfaced battery energy storage systems on frequency regulation in low-inertia power grids," *Sustainable Energy, Grids and Networks*, vol. 27, p. 100496, 2021, ISSN: 2352-4677. DOI: <https://doi.org/10.1016/j.segan.2021.100496>. [Online]. Available: <https://www.sciencedirect.com/science/article/pii/S2352467721000679>.
- [52] L. Harnefors, *Control of power electronic converters and variable-speed drives*.
- [53] R. Rosso, X. Wang, M. Liserre, X. Lu, and S. Engelken, "Grid-forming converters: An overview of control approaches and future trends," in *2020 IEEE Energy Conversion Congress and Exposition (ECCE)*, 2020, pp. 4292–4299. DOI: 10.1109/ECCE44975.2020.9236211.
- [54] L. Zhang, L. Harnefors, and H.-P. Nee, "Power-synchronization control of grid-connected voltage-source converters," *IEEE Transactions on Power Systems*, vol. 25, no. 2, pp. 809–820, 2010. DOI: 10.1109/TPWRS.2009.2032231.
- [55] L. Harnefors, M. Hinkkanen, U. Riaz, F. M. M. Rahman, and L. Zhang, "Robust analytic design of power-synchronization control," *IEEE Transactions on Industrial Electronics*, vol. 66, no. 8, pp. 5810–5819, 2019. DOI: 10.1109/TIE.2018.2874584.
- [56] U. Tamrakar, D. Shrestha, M. Maharjan, B. P. Bhattarai, T. M. Hansen, and R. Tonkoski, "Virtual inertia: Current trends and future directions," *Applied Sciences*, vol. 7, no. 7, 2017, ISSN: 2076-3417. DOI: 10.3390/app7070654. [Online]. Available: <https://www.mdpi.com/2076-3417/7/7/654>.

- [57] S. D'Arco, J. A. Suul, and O. B. Fosso, "A virtual synchronous machine implementation for distributed control of power converters in smartgrids," *Electric Power Systems Research*, vol. 122, pp. 180–197, 2015, ISSN: 0378-7796. DOI: <https://doi.org/10.1016/j.epsr.2015.01.001>. [Online]. Available: <https://www.sciencedirect.com/science/article/pii/S0378779615000024>.
- [58] A. Narula, M. Bongiorno, M. Beza, J. R. Svensson, X. Guillaud, and L. Harnefors, "Impact of steady-state grid-frequency deviations on the performance of grid-forming converter control strategies," in *2020 22nd European Conference on Power Electronics and Applications (EPE'20 ECCE Europe)*, 2020, P.1–P.10. DOI: [10.23919/EPE20ECCEEurope43536.2020.9215947](https://doi.org/10.23919/EPE20ECCEEurope43536.2020.9215947).
- [59] M. G. Taul, X. Wang, P. Davari, and F. Blaabjerg, "Current limiting control with enhanced dynamics of grid-forming converters during fault conditions," *IEEE Journal of Emerging and Selected Topics in Power Electronics*, vol. 8, no. 2, pp. 1062–1073, 2020. DOI: [10.1109/JESTPE.2019.2931477](https://doi.org/10.1109/JESTPE.2019.2931477).
- [60] A. Narula, M. Bongiorno, M. Beza, and P. Chen, "Tuning and evaluation of grid-forming converters for grid-support," in *2021 23rd European Conference on Power Electronics and Applications (EPE'21 ECCE Europe)*, 2021, P.1–P.10.
- [61] L. Zhang, H. Peng, Z. Ning, M. Zhongqiang, and C.-Y. Sun, "Comparative research on rc equivalent circuit models for lithium-ion batteries of electric vehicles," *Applied Sciences*, vol. 7, p. 1002, Sep. 2017. DOI: [10.3390/app7101002](https://doi.org/10.3390/app7101002).
- [62] M.-K. Tran, M. Mathew, S. Janhunen, S. Panchal, K. Raahemifar, R. Fraser, and M. Fowler, "A comprehensive equivalent circuit model for lithium-ion batteries, incorporating the effects of state of health, state of charge, and temperature on model parameters," *Journal of Energy Storage*, vol. 43, p. 103252, 2021, ISSN: 2352-152X. DOI: <https://doi.org/10.1016/j.est.2021.103252>. [Online]. Available: <https://www.sciencedirect.com/science/article/pii/S2352152X2100949X>.
- [63] C. J. O'Rourke, M. M. Qasim, M. R. Overlin, and J. L. Kirtley, "A geometric interpretation of reference frames and transformations: Dq0, clarke, and park," *IEEE Transactions on Energy Conversion*, vol. 34, no. 4, pp. 2070–2083, 2019. DOI: [10.1109/TEC.2019.2941175](https://doi.org/10.1109/TEC.2019.2941175).
- [64] M. Nagpal, A. Moshref, G. Morison, and P. Kundur, "Experience with testing and modeling of gas turbines," in *2001 IEEE Power Engineering Society Winter Meeting. Conference Proceedings (Cat. No.01CH37194)*, vol. 2, 2001, 652–656 vol.2. DOI: [10.1109/PESW.2001.916931](https://doi.org/10.1109/PESW.2001.916931).
- [65] M. Sabbouh, *Personal communication*, May 2022.

A

Rya Gas Turbine Verification

In order to verify that the gas turbines of Rya CHP plant function as intended, the power plant is connected by itself to supply a constant load. A simplified load rejection is applied in order to analyze the frequency and power response characteristics of the gas turbines. The response is then compared to available measurements and tests that have been performed on real gas turbines [64]. The resulting active power exchange and the corresponding frequency response when the generator is set to dispatch 100 MW with a load rejection of 15 MW at five seconds is shown in Figure A.1. It can be seen that the frequency sees an oscillation before finding a new steady state of operation. The result is a slight increase in frequency as expected due to the loss of load to supply, agreeing with the expected result from the swing equation and the results from [64].

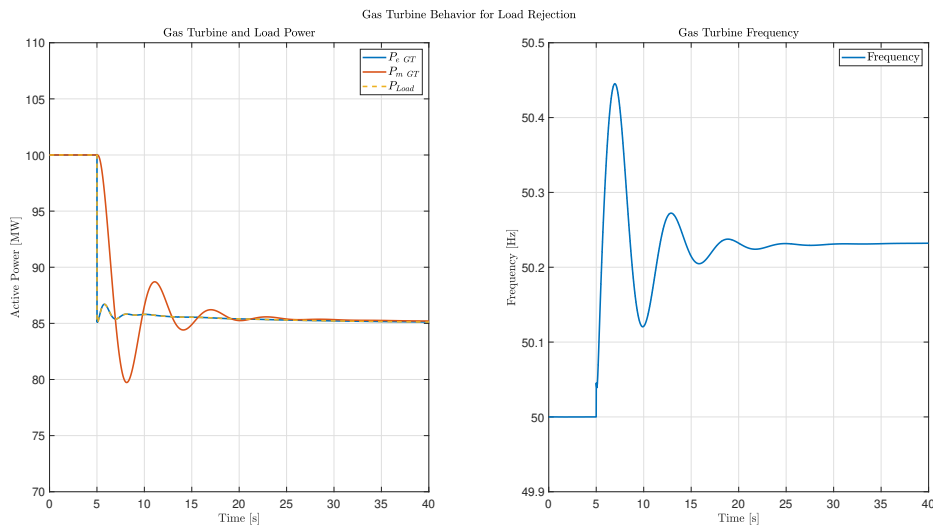


Figure A.1: Active power output for gas turbine and load active power, as well as system frequency. Initially, the gas turbine is supplying a load of 100 MW, and at the time of 5 seconds, 15 MW load is suddenly lost, causing the gas turbine to reduce its output active power and increase the corresponding frequency.

DEPARTMENT OF ELECTRICAL ENGINEERING
CHALMERS UNIVERSITY OF TECHNOLOGY
Gothenburg, Sweden
www.chalmers.se



CHALMERS
UNIVERSITY OF TECHNOLOGY